Molecular Biology of the Cell
Vol. 7, 917–934, June 1996

Pleiotropic Nuclear Defects Associated with a Conditional Allele of the Novel Nucleoporin Rat9p/Nup85p

Alan L. Goldstein,* Christine A. Snay, Catherine V. Heath, and Charles N. Cole†

Department of Biochemistry, Dartmouth Medical School, Hanover, New Hampshire 03755

Submitted November 14, 1995; Accepted March 28, 1996
Monitoring Editor: David Botstein

In a screen for mutants defective in nucleocytoplasmic export of mRNA, we have identified a new component of the *Saccharomyces cerevisiae* nuclear pore complex (NPC). The *RAT9/NUP85* (ribonucleic acid trafficking) gene encodes an 84.9-kDa protein that we have localized to NPCs by tagging the *RAT9/NUP85* gene with the in vivo molecular marker Green Fluorescent Protein. In cells containing either the *rat9–1* allele or a complete deletion of the *RAT9/NUP85* gene, poly(A)$^+$ RNA accumulates rapidly in nuclei after a shift from 23°C to 37°C. Under these same conditions, rapid fragmentation of the nucleolus was also observed. At the permissive growth temperature in *rat9–1* or *RAT9* deletion strains, the nuclear envelope (NE) becomes detached from the main body of the nucleus, forming long thin double sheets of NE. NPCs within these sheets are clustered and some appear to be locked together between opposing sheets of NE such that their nucleoplasmic faces are in contact. The Rat9/Nup85 protein could not be detected in cells carrying a mutation of *RAT2/NUP120*, suggesting that Rat9p/Nup85p cannot be assembled into NPCs in the absence of Rat2p/Nup120p. In contrast, Rat9/Nup85 protein was readily incorporated into NPCs in strains carrying mutant alleles of other nucleoporin genes. The possible role of Rat9p/Nup85p in NE integrity and the loss of nucleoporins when another nucleoporin is mutant or absent are discussed.

INTRODUCTION

The export of mature molecules of messenger RNA from the nucleus to the cytoplasm is an essential step in gene expression. Once pre-mRNAs are transcribed and processed they are delivered to the cytoplasm in the form of ribonucleoprotein particles (RNP) in a multi-step process. In the first step, RNPs move from their sites of transcription and processing to the nuclear envelope (NE). Whether messenger RNPs are transported to the NE attached to the nucleoskeleton or arrive there by diffusion is uncertain and is a current subject of debate (for review, see Rosbash and Singer, 1993). By analogy with the steps of nuclear protein import, mRNPs presumably bind at sites on the nuclear face of nuclear pore complexes (NPCs) and are subsequently translocated through the central channel of the NPC.

NPCs are proteinacious organelles of approximately 124 megadaltons (mDa) capable of transporting substrates with diameters of up to 230 Å (Feldherr *et al.*, 1984; Reichelt *et al.*, 1990). Traffic through NPCs is bi-directional with many proteins and some RNAs (e.g. snRNPs) traveling in the inbound direction, and RNPs and some proteins traveling in the outbound direction (Feldherr *et al.*, 1984; Dworetzky and Feldherr, 1988). Protein traffic through the NPC requires, and is presumably regulated by, a GTPase cycle using the small GTPase, Ran/TC4 (Melchior *et al.*, 1993; Moore and Blobel, 1993). Since mRNA is exported in the form of mRNPs and nuclear protein export requires Ran-mediated GTP hydrolysis (Moroianu and Blobel, 1995), it seems probable that mRNA export also requires the activity of Ran/TC4.

* Present address: P.O. Box 132, Lincoln University, Canterbury, New Zealand.
† Corresponding author.

NPCs are estimated to contain 75–100 different proteins, called nucleoporins (Forbes, 1992; Rout and Blobel, 1993). Fewer than two dozen yeast NPC proteins, and a smaller number from vertebrate organisms, have been isolated and characterized. Approximately half of the yeast nucleoporins so far identified contain one or more classes of peptide repeats consisting of either GLFG, XFXFG, or XXFG (reviewed in Rout and Wente, 1994). The repeat domains of individual nucleoporins are often dispensable, probably due to their redundancy among different nucleoporins that contain the same class of repeat (Wente *et al.*, 1992; Fabre *et al.*, 1994). Recent data indicate that the repeat domains of several different nucleoporins can function as docking sites for transport substrate (Kraemer *et al.*, 1995; Radu *et al.*, 1995; Wu *et al.*, 1995). Radu *et al.* (1995) have proposed that bi-directional transport through the NPC occurs by guided diffusion, with the substrate docking and undocking at multiple sites along the axis of the NPC.

In this report we describe a novel yeast nucleoporin identified in a screen for mutants with conditional defects in mRNA export. We cloned *RAT9/NUP85* (Ribonucleic Acid Trafficking) by complementation of the temperature-sensitive growth defect of a mutant *Saccharomyces cerevisiae* strain. The *RAT9/NUP85* gene encodes an 84.9 kDa-protein, Rat9p/Nup85p, that lacks repeat motifs. Strains with either the *rat9–1* allele or a disruption of *RAT9/NUP85* had nearly identical phenotypes that include temperature-sensitive growth, a rapid block in mRNA export, and concomitant fragmentation of the nucleolus following a shift of cells to 37°C. These strains also displayed constitutive defects in NPC distribution and NE morphology. Interestingly, we were unable to detect the Rat9/Nup85 protein in cells carrying a mutation of *RAT2/NUP120*, suggesting that Rat9p/Nup85p cannot be assembled into NPCs in the absence of Rat2p/Nup120p.

MATERIALS AND METHODS

Yeast Strains, Media, Genetic Methods, and Mutant Isolation

Table 1 lists the strains and plasmids used in this study. The *S. cerevisiae* strains were derived from strains FY23 and FY86 (provided by Dr. Fred Winston, Harvard Medical School, Boston, MA). Yeast strains were grown in rich media (YPD) or synthetic complete media lacking specific amino acids (SC-dropout) using standard recipes (Rose *et al.*, 1989). Matings, sporulations, tetrad analysis, and transformations were performed using standard protocols (Guthrie and Fink, 1991).

We isolated AGY195, a mutant yeast strain bearing a temperature-sensitive allele of *RAT9*, in a screen for mRNA export mutants that has been described previously (Amberg *et al.*, 1992; Gorsch *et al.*, 1995). Briefly, a collection of 1200 temperature-sensitive strains were generated by mutagenesis with UV light. Pools of these strains were grown to mid-log phase at 23°C and then shifted to 37°C for 2 h before being harvested and processed for fluorescent in situ hybridization (FISH) to examine the subcellular location of poly(A)$^+$ RNA. Positive pools (those that contained cells exhibiting accumulation of fluorescent signal within their nuclei) were broken down and each strain was retested individually.

FISH Assay Immunochemical Methods

To localize poly(A)$^+$ RNA in yeast cells we used a previously described FISH assay (Amberg *et al.*, 1992). The probe in this assay was digoxigenated oligo(dT)$_{50}$ that hybridizes to the poly(A) tail of mRNAs. The amount of probe used for individual assays was determined empirically for each batch of probe prepared. In general, we used about 8 μg of probe per 300 μl of hybridization solution. To visualize the sites at which the probe hybridized, fluorescein isothiocyanate (FITC)-labeled anti-digoxigenin antibody (Boehringer Mannheim Biochemicals, Indianapolis, IN) was used at between 1:10 and 1:50 dilution. Previous control studies showed that the anti-digoxigenin signal is specific for poly(A)$^+$ RNA and requires active RNA polymerase II transcription (Amberg *et al.*, 1992). The nuclear region of yeast cells was identified by counterstaining cells with 4′,6-diamidino-2-phenylindole-dihydrochloride (DAPI), a DNA-binding dye.

Indirect immunofluorescence was performed as previously described (Mirzayan *et al.*, 1992; Copeland and Snyder, 1993). To identify the nucleolus we used either anti-Nsr1p mAb 2.3B (provided by Dr. M. Snyder, Yale University, New Haven, CT) at a 1:10 dilution or anti-Nop1p mAB A66 (Aris and Blobel, 1988; provided by Dr. J. Aris, University of Florida, Gainesville, FL) at a 1:100 dilution. NPCs were localized using either anti-Rat7p/Nup159p antibody (prepared in guinea pigs) (Gorsch *et al.*, 1995) at a 1:2000 dilution or mAb RL1 (Snow *et al.*, 1987; provided by Dr. L. Gerace, Scripps Research Institute, La Jolla, CA) at a 1:400 dilution. RL1 is a monoclonal antibody raised against rat liver NEs and recognizes multiple NPC proteins in both yeast and mammalian cells (Snow *et al.*, 1987; Copeland and Snyder, 1993). We used either FITC- or Texas Red-conjugated species-specific secondary antibodies (Vector Labs, Burlingame, CA) at 1:650 dilution to visualize the sites at which primary antibodies were bound. To examine the co-localization of Rat9p and NCP, cells were stained with both the anti-myc epitope monoclonal antibody and with RL1. The anti-"myc" antibody is an immunoglobulin G (IgG), whereas the RL1 antibody is an IgM. Secondary antibodies, horse anti-mouse IgG coupled to FITC, and goat anti-mouse IgM coupled to Texas Red (both from Vector Labs) were used at 1:500 and 1:650 dilution, respectively.

To analyze myc-epitope tagged proteins by Western blot, yeast cells in 5-ml cultures were harvested by low speed centrifugation, and the cells broken open by boiling and vortexing in the presence of glass beads and SDS/urea sample buffer. The cell lysates were separated by SDS/PAGE, blotted to polyvinylidene difluoride membrane (Bio-Rad, Hercules, CA), and probed with 10 μg/ml of anti-myc 9E10 antibody (Oncogene Sciences, Uniondale, NY).

Electron Microscopy

S. cerevisiae were examined by electron microscopy using the following previously described protocol (Byers and Goetsch, 1975; Wright and Rhine, 1989). The cells were grown to an OD$_{600}$ of 1 in YPD media, pelleted, and resuspended in 0.1 M cacodylate buffer (pH 6.8). Primary fixation was done with 3% glutaraldehyde and 0.1% tannic acid in 0.1 M cacodylate buffer (pH 6.8) at room temperature for 2 h. Cells were washed twice with 0.05 M phosphate buffer (pH 7.5) and spheroplasted with 30–60 μg of Zymolyase 100T (Seikagaku America, Rockville, MD) per milliliter. After washing with cacodylate buffer (pH 6.8) the cells were embedded in low melting temperature agarose (SeaPrep; FMC, Bioproduct, Rockland, ME). Post fixation was carried out with 2% osmium tetroxide in 0.1 M cacodylate buffer (pH 6.8) for 1 h on ice. Subsequently, the cells were washed in cacodylate buffer (pH

Table 1. Yeast strains and plasmids

	Genotype/description	Source
Yeast strains		
FY23	*Mata ura3-52 leu2Δ1 trp1Δ63*	F. Winston
ACY1	*Mata/Matα ura3-52/ura3-52 leu2/Δ1/leu2Δ1 trp1Δ63/TRP his3Δ200/his3Δ200*	Dr. Anita Corbett
ACY2	*Mata/Matα ura3-52/ura3-52 leu2Δ1/leu2Δ1 trp1Δ63/trp1Δ63 his3Δ200/his3Δ200*	Dr. Anita Corbett
AGY195.204A	*Matα ura3-52 leu2Δ1 trp1Δ63 rat9-1/nup85-1*	This study
AGY401	*Matα ura3-52 leu2Δ1 trp1Δ63 rat9-1/nup85-1*	This study
AGY402	*Mata ura3-52 leu2Δ1 his3Δ200 rat9-1/nup85-1*	This study
AGY902	*Mata/Matα ura3-52/ura3-52 leu2/Δ1/leu2Δ1 trp1Δ63/trp1Δ63 his3Δ200/his3Δ200 RAT9/RAT9::HIS3*	This study
AGY904	*Mata/Matα ura3-52/ura3-52 leu2/Δ1/leu2Δ1 trp1Δ63/trp1Δ63 his3Δ200/his3Δ200 RAT9/RAT9::HIS3 pRAT9.3 (URA3 RAT9 CEN)*	This study
AGY908	*Mata ura3-52 leu2Δ1 trp1Δ63 his3Δ200 RAT9::HIS3*	This study
AGY909	*Mata ura3-52 leu2Δ1 trp1Δ63 his3Δ200 RAT9::HIS3 pRAT9.25 (TRP1 CEN RAT9$_{myc}$)*	This study
AGY910	*Mata ura3-52 leu2Δ1 trp1Δ63 his3Δ200 RAT9::HIS3 pRAT9.30 (TRP1 CEN rat9-1$_{myc}$)*	This study
AGY911	*Mata ura3-52 trp1Δ63 leu2Δ1 pRAT9.28 (TRP1 CEN RAT9$_{GFP}$)*	This study
AGY912	*Mata ura3-52 leu2Δ1 trp1Δ63 his3Δ200 RAT9::HIS3 pRAT9.28 (TRP1 CEN RAT9$_{GFP}$)*	This study
AGY913	*Mata ura3-52 trp1Δ63 leu2Δ1 rat2-1/nup120-1 pRAT9.28 (TRP1 CEN RAT9$_{GFP}$)*	This study
AGY914	*Mata ura3-52 trp1Δ63 leu2Δ1 rat2-1/nup120-1 pRAT9.25 (TRP1 CEN rat9-1$_{myc}$)*	This study
AGY917	*Matα ura3-52 leu2Δ1 his3Δ200 RAT9::HIS3*	This study
CCY1	*Mata ura3-52 trp1Δ63 leu2Δ1 prp20-1*	Dr. Anita Corbett
CCY282	*Mata ura3-52 trp1Δ63 leu2Δ1 rat2-1/nup120-1*	Cole Lab
CHY104	*Mata ura3-52 his3Δ200 leu2Δ1 RAT2/NUP120::HIS3*	Cole Lab
CHY109	*Mata ura3-52 trp1Δ63 leu2Δ1 rat2-1/nup120-1 pCH12 (LEU2 CENRAT2$_{myc}$)*	Cole Lab
CHY110	*Mata ura3-52 trp1Δ63 leu2Δ1 rat2-1/nup120-1 pRAT9.25 (TRP1 CEN RAT9$_{myc}$)*	This study
CHY111	*MAT URA3-52 TRP163 LEU21 RAT2-11 NUP120-1 PRAT9.25 (TRP1 CEN RAT9myc)*	This study
CSY501	*Matα ura3-52 leu2Δ1 his3Δ200 RAT9::HIS3 pRAT9.3 (URA3 CEN RAT9)*	This study
LGY103	*Mata ura3-32 leu2Δ1 trp1Δ63 rat7-1/nup159-1*	
LGY112	*Mata ura3-52 leu2Δ1 his3Δ200 rat7-1/nup159-1*	Cole Lab
OLY104	*Mata ura3-52 leu2Δ1 his3Δ200 RAT3/NUP133::HIS3*	Cole Lab
OLY109	*Matα, ura3-52, leu2Δ1, trp1Δ63 rat3-1/nup133-1*	
OLY114	*Mata ura3-52 leu2Δ1 trp1Δ63 rat3-1/nup133-1 pOL1(RAT3 URA3 CEN)*	Cole Lab
TDY105	*Mata ura3-52 leu2Δ1 trp1Δ63 nup145-10*	Cole Lab
Plasmids		
pRAT9.1-9.6	Original complementing clones, URA3 CEN (from Rose library; Rose *et al.*, 1987)	
pAG55	5-kb *XbaI* fragment from pRAT9.4 subcloned into pMOB1	
pRAT9.15	3.5-kb *XbaI* to *EcoRV* fragment from pAG55 subcloned into YCplac22 (Gietz and Sugino, 1988) TRP1 CEN	
pRAT9.16	*ClaI* fragment dropped out of pRAT9.15	
pRAT9.25	3X myc-epitope subcloned into *ClaI* site of pRAT9.16	
pRAT9.26	gap-repaired plasmid from *StuI-AgeI* digestion of pRAT9.15	
pRAT9.27	gap-repaired plasmid from *AgeI-Eco47III* digestion of pRAT9.15	
pRAT9.28	GFP-S65T subcloned into *ClaI* site of pRAT9.16	
pRAT9.30	*NcoI–Eco47III* fragment from pRAT9.27 subcloned into same sites of pRAT9.25	

6.8), deionized water, stained en bloc with 0.5% uranyl acetate overnight, dehydrated with ethanol and acetone, and embedded in Spurr's resin (medium grade). Thin sections were cut on a Sorvall MT5000 ultramicrotome with a section thickness of 90 nm. Sections were post stained with uranyl acetate and Venable and Coggleshell's lead citrate and examined on a JEOL 100CX electron microscope at 80 kV.

Cloning, Mapping, and Sequencing RAT9

To clone the wild-type *RAT9* gene, we transformed logarhythmically growing AGY402 cells by electroporation with a wild-type yeast genomic library (Rose *et al.*, 1987). This library was constructed by subcloning 10- to 30-kbp *Sau3* A partial digestion fragments from a S288C-derived yeast strain into a *CEN-URA3* shuttle vector. The transformed cells were plated onto SC-URA plates and incubated at 37°C to select for complementing clones. Plasmid DNA from six colonies that grew at 37°C was purified (Rose *et al.*, 1989) and the recovered plasmids were transformed into the *Escherichia coli* strain DH5α. We digested these plasmids (pRAT9.1–pRAT9.6) with *DraI* and found that all six were closely related. To show that the yeast colonies from which the plasmids were isolated were not revertants, the purified plasmids were retransformed back into AGY402 and tested for growth at 37°C and mRNA export competence by FISH.

The *RAT9* gene was sequenced using the Gold Biotechnology TN1000 system (St. Louis, MO). This system is based upon transposon mutagenesis of target DNA (Strathmann *et al.*, 1991). Sequence data is obtained by using primers complementary to the ends of the transposon and sequencing into the target DNA. We subcloned a 5-kbp *XbaI* fragment from pRAT9.4 into the transposon target vector pMOB to obtain pAG55, and created transposon mutants following the manufacturers' instructions. Sequencing template was generated using the PRISM dideoxy sequencing kit (ABI, Foster City, CA) and the reactions were run on an ABI 373A DNA Sequencer (ABI). We ordered the DNA sequence into three large contigs and were able to sequence across each gap with primers complementary to the ends of the contigs.

Isolation of the rat9–1 Allele

The mutation of the *rat9–1* allele was cloned by gap-repair (Rothstein, 1991). In this procedure the mutation is recovered by transforming a mutant yeast strain with a linear plasmid that has had a section of the corresponding wild-type gene removed by restriction endonuclease digestion. The gapped molecule uses the chromosomal copy of the gene to repair the gap. If the gapped region spans the site of the mutation, the resulting repaired plasmid will bear a mutant copy of the gene; otherwise, the repaired plasmid will contain a wild-type version of the gene. The phenotype of the strain is then tested to determine whether the extrachromosomal copy of the gene on the plasmid is wild type or mutant. To locate the mutation in *rat9–1*, we made four different gaps by deleting the following fragments of the *RAT9* gene: *Cla*I (97) to *Nco*I (516), *Nco*I (516) to *Stu*I (843), *Stu*I (843) to *Age* I (1294), and *Age* I (1294) to *Eco47* III (2010). The linear fragments were gel purified and 1 μg of each was transformed separately into AGY401 (containing *rat9–1*) by electroporation. The recipient strain is auxotrophic for tryptophan while the gapped plasmids contain the *TRP1* gene. We selected for repair of the plasmids by plating the transformed cells onto SC-TRP plates and tested colonies that appeared on these plates to determine if they grew at 37°C. Plasmids were recovered from strains that could not grow at 37°C and the mutation was identified by sequencing. The plasmids resulting from gap-repair of two of the gapped plasmids conferred growth at 37°C (*Cla*I to *Nco*I and *Nco*I to *Stu*I) and two did not. We interpreted this result to mean that the mutation lay between *Stu*I and *Eco47* III and might be close to the junction between these two gaps, that is, close to the *Age* I site.

The *Stu*I to *Age* I and *Age* I to *Eco47* III gap-repaired plasmids were recovered and the *rat9–1* mutation was identified by sequencing. Using primers upstream and downstream of the *Age* I site, we sequenced both strands of pRAT9.15 (containing wild-type *RAT9*), pRAT9.26 (*Stu*I to *Age* I gap repair), and pRAT9.27 (*Age* I to *Eco47* III gap repair).

Deletion of the RAT9 Gene and Testing for Essentiality of RAT9

To delete the *RAT9* gene we used a polymerase chain reaction (PCR)-based gene deletion approach (Baudin *et al.*, 1993). By PCR amplification we generated a *HIS3* gene that was flanked at its ends by 45 nucleotides identical to sequences just upstream and downstream of the *RAT9* open reading frame (ORF). The sequence of the upstream oligo was 5′ ATATATCCTAATATACCATCCGAAGGACATTACTATACTGATTTAGGCCTCCTCTAGTACACTC 3′ and the sequence of the downstream oligo was 5′ CTTGAGTTGAGTCAATAAGCGTGAGCCAGAACGCAATTATCAGATGCGCGCCTCGTTCAGAATG 3′. For both oligos, the last 17 nucleotides are homologous to the *HIS3*-selectable marker. To generate the deletion construct, 20 ng of the HIS3-containing plasmid pBM2815 (obtained from P. Silver, Dana-Farber Cancer Institute, Boston, MA), was used as the template in a 50-μl PCR reaction containing 1× PCR buffer (10 mM Tris-HCl, 15 mM $MgCl_2$, 50 mM KCl, 100 μg/ml gelatin; pH 8.3), 0.8 mM dNTP (0.2 mM each dATP, dGTP, dCTP, and dTTP), 1 μM each upstream and downstream oligos, and 2 U *Taq* DNA polymerase (Boehringer Mannheim Biochemicals). The reaction was subjected to a 30-cycle amplification consisting of 1.5 min at 94°C, 2.0 min at 50°C, and 2.0 min at 72°C. The PCR product was purified and transformed into the wild-type diploid strains ACY1 and ACY2, both homozygous for *his3Δ200*. The flanking upstream and downstream sequences target the deletion construct to the *RAT9* locus such that the *RAT9* ORF is replaced with *HIS3* by homologous recombination. Recombinants were selected by plating the transformed cells on SC-HIS plates. Homologous recombination at this locus in two His^+ colonies was verified by Southern blot analysis.

To determine whether Rat9p is essential for vegetative growth, we transformed the diploid carrying *HIS3* in place of one of the *RAT9* genes (AGY902) with pRAT9.2, one of the complementing plasmids obtained while cloning *RAT9*. pRAT9.2 contains the *URA3* gene that allows counterselection against the plasmid by growth on 5-fluoro-orotic acid (5-FOA) plates (Boeke *et al.*, 1987). We sporulated the resulting transformants, dissected tetrads, and scored four-spore tetrads for their ability to grow on 5-FOA plates and for auxotrophic markers.

Epitope Tagging RAT9 and rat9–1

We tagged Rat9p with Green Fluorescent Protein-S65T (GFP) (Heim *et al.*, 1995) and separately with three consecutive myc epitopes (3× myc) (the epitope is EQKLISEEDLN). To subclone the epitopes into *RAT9*, we first constructed pRAT9.16 by deleting the 13-nucleotide *Cla*I fragment from pRAT9.15 (*RAT9 TRP1 CEN*). This creates a frame-shift near the 5′ end of *RAT9* such that pRAT9.16 does not complement the temperature-sensitive growth defect of *rat9* strains at 37°C. We next PCR amplified the epitopes so they could be subcloned in-frame into the *Cla*I site of pRAT9.16, restoring the *RAT9* reading frame. The PCR reaction conditions for amplifying GFP-S65T and 3× myc were the same as those described for amplifying the *HIS3* gene in the previous section. The GFP tag was made by using the oligos 5′- CCGGATCGATAGTAAAGGAGAAGAAC-3′ and 5′-GGCGCTGGTGCTGGTGCTGATCGATTTAA-3′ to amplify GFP within pZA66 (provided by M. Moser, University of Washington, Seattle, WA). These oligos contain *Cla*I sites flanking the GFP sequence. The 3× myc tag was made using the oligos 5′-TATAGGCGCCTCCTCTAGAGGTGAAC-3′ and 5′-TTAAGGCGCCCGACTCTAGAGGATCC-3′ to amplify the triple myc epitope from pKK-1 (provided by Dr. G. Fink, Massachusetts Institute of Technology, Cambridge, MA). These oligos contain *Nar*I sites that have ends compatible with *Cla*I. After digesting and ligating the PCR products and pRAT9.16, the ligations were transformed directly into the *RAT9* deletion strain AGY908. Transformants containing functional Rat9p-GFP or Rat9p-myc were selected on SC-TRP plates incubated at 37°C. To epitope tag the *rat9–1* allele with 3× myc, we subcloned an *Nco*I–*Eco47* III fragment containing the *rat9–1* mutation from the gap-repaired plasmid pRAT9.26 into the same sites of pRAT9.25 (RAT9p-myc).

Microscopy and Imaging

For fluorescence microscopy we used a Zeiss Axiophot microscope, captured images with a CH250 cooled CCD camera (Photometrics, Tucson, AZ), and processed the data with BDS Image Version 1.5 (Oncor Imaging Systems, Rockville, MD). Confocal data was gathered with a Bio-Rad MRC1000 confocal system using a Krypton KR/AR 15 mW laser mounted on a Zeiss Axioskop microscope using Comos Version 6.05.8 (Bio-Rad) to process the data. We used Adobe Photoshop Version 3.05 to prepare the micrographs for illustrations.

Synthetic Lethality

To test whether a disruption of *RAT9* was synthetically lethal with mutant alleles of other nucleoporins, diploids heterozygous for two mutations of interest were obtained by mating appropriate strains. CSY501 (disruption of *RAT9*) was mated with LGY112 (carrying the *rat7–1/nup159–1* allele), TDY105 (carrying the *nup145–10* allele), OLY104 (carrying a disruption of *RAT3/NUP133*), OLY114 (carrying the *rat3–1/nup133–1* allele), or CHY104 (carrying a disruption of *RAT2/NUP120*). Heterozygous diploids all contained the wild-type *RAT9* gene and *URA3* on a centromere-based plasmid. Diploids were sporulated, dissected, and haploid progeny evaluated for their ability to grow on media lacking uracil, histidine, or tryptophan. By plating on 5-FOA, the requirement for the plasmid-borne copy of *RAT9* was tested. We also evaluated the ability of haploids able to grow on 5-FOA for their ability to grow at 37°C. Of the 10 four-spore tetrads analyzed following sporulation of the strain heterozygous for a disruption of *RAT9* and carrying the *rat7–1/nup159–1* allele, the

ratio of those yielding two, three, or four haploids able to grow on 5-FOA plates was 4:5:1. For the 4 four-spore tetrads analyzed following sporulation of the strain heterozygous for disruptions of both *RAT9* and of *RAT3/NUP133*, one of the four haploids from each tetrad was unable to grow on 5-FOA. From the 8 four-spore tetrads analyzed following sporulation of the strain heterozygous for a disruption of *RAT9* and carrying the *rat3–1/nup133–1* allele, the ratio of those yielding two, three, or four haploids able to grow on 5-FOA was 0:6:2. For the 9 four-spore tetrads analyzed following sporulation of the strain heterozygous for a disruption of *RAT9* and carrying the *nup145–10* allele, the ratio of those yielding two, three, or four haploids able to grow on 5-FOA was 4:5:0. In almost all cases where only two haploids could grow on 5-FOA, those strains were not temperature sensitive. In almost all cases where three haploids could grow on 5-FOA, two of the three were temperature sensitive. In almost all cases where four haploids could grow on 5-FOA, all four were temperature sensitive. The segregation of all of the other markers was as expected. These ratios and patterns are close to those theoretically predicted to be obtained if the disruption of *RAT9* were synthetically lethal with the mutations tested that affect other nucleoporins. We were unable to obtain sporulation of the diploid heterozygous for disruption of both *RAT9* and *RAT2/NUP120*, regardless of whether the strain contained a wild-type plasmid-borne copy of *RAT9* or *RAT2/NUP120*.

RESULTS

Cells Bearing the rat9–1 Mutation Display a Rapid Block in mRNA Export and Stop Growing when Shifted to 37°C

The subject of this report is the *RAT9/NUP85* gene (Ribonucleic Acid Trafficking) and strains bearing mutant alleles of this gene. The AGY195 strain carrying the *rat9–1* mutant allele was obtained in a previously described screen for mRNA export mutants (Amberg *et al.*, 1992; Gorsch *et al.*, 1995). Briefly, a collection of approximately 1,200 heat-sensitive yeast strains were constructed and screened by FISH to identify strains that accumulated poly(A)$^+$ RNA within the nucleus when shifted to the nonpermissive temperature of 37°C. The oligonucleotide probe used to detect the poly(A) tail of mRNA was digoxigenated oligo(dT)$_{50}$, which was visualized using an FITC-conjugated anti-digoxigenin antibody. The nuclear region of the cells was identified by counterstaining the cells with the DNA binding dye, DAPI. Putative mutants were genetically characterized to identify those strains in which a single recessive mutation was responsible for both the accumulation of poly(A)$^+$ RNA in nuclei and the inability to grow after a shift to 37°C. The mutants were then sorted into complementation groups by crossing the strains in pairs and testing the resulting diploids for growth at 37°C. Along with the *rat9–1* strain, we obtained nine other new complementation groups from this screen and new alleles of *PRP20* and *RNA1*.

Figure 1 illustrates the mRNA localization pattern of wild-type and *rat9–1* cells determined by FISH. Wild-type cells (FY23) grown at 37°C had uniform fluorescent staining throughout the cell, which indicates that mRNA export is an efficient process (Figure 1A). Wild-type cells grown at 23°C looked the same as those grown at 37°C (our unpublished results). *rat9–1* cells (AGY401) grown at 23°C had a variety of mRNA localization patterns (Figure 1D). Some cells appeared to have wild-type distribution of mRNA while others had varying levels of nuclear poly(A)$^+$ RNA accumulation. We examined the distribution of poly(A)$^+$ RNA in *rat9–1* cells grown continuously at different temperatures between 17°C and 25°C and did not find a temperature where all the cells appeared wild type. Instead, we saw a correlation between the amount of nuclear poly(A)$^+$ RNA and the temperature of incubation (our unpublished results). When *rat9–1* cells were shifted from 23°C to 37°C for periods as short as 15 min, nuclear accumulation of poly(A)$^+$ RNA was seen in most cells, and after 1 h, a dramatically enhanced accumulation of poly(A)$^+$ RNA was seen within the nucleus of every cell (Figure 1G). Following a shift to 37°C, cell division ceased rapidly, and within 4 h after the culture was shifted, 25% of the cells had become nonviable (Figure 2). A 24-h incubation period at 37°C resulted in almost complete lethality.

Nuclear Structural Defects in rat9–1 Cells

NPCs are usually distributed relatively uniformly around the NE in yeast cells. Mutation or deletion of several yeast nucleoporins results in clustering of NPCs within the NE (Wente *et al.*, 1992; Wente and Blobel, 1993, 1994; Doye *et al.*, 1994; Gorsch *et al.*, 1995; Heath *et al.*, 1995; Li *et al.*, 1995). Therefore, we examined the distribution of NPCs in *rat9–1* cells by indirect immunofluorescence. NPCs were localized with either polyclonal guinea pig antiserum raised against the nucleoporin Rat7p/Nup159p (Gorsch *et al.*, 1995) or mAb RL1 that recognizes several yeast NPC proteins (Snow *et al.*, 1987). Figure 3A shows wild-type cells (FY23) grown at 23°C with typical punctate rim staining of the nucleus. When we examined the distribution of NPCs in *rat9–1* cells (AG401) grown at 23°C we saw that most of the cells had NPCs clustered at one point or in a crescent along the edge of the NE (Figure 3C). In some cells we saw disorganized patches of NPCs. We did not see any additional changes in NPC distribution in *rat9–1* cells shifted to 37°C for periods up to 4 h (our unpublished results).

To corroborate our immunofluorescence data, we examined wild-type and *rat9–1* cells by thin-section electron microscopy. To visualize NPCs we counterstained 90-nm-thick sections with uranyl acetate and lead citrate. Figure 4A shows a wild-type cell grown at 37°C, revealing NPCs distributed around the NE, while Figure 4, A, B, C, and F, show *rat9–1* cells grown at 23°C and Figure 4, D and E, show *rat9-1* cells grown at 37°C. The *rat9–1* cells show clustered NPCs. In typical thin sections we could see about 8–12 nuclear pores in a cluster and two to three NPCs located away

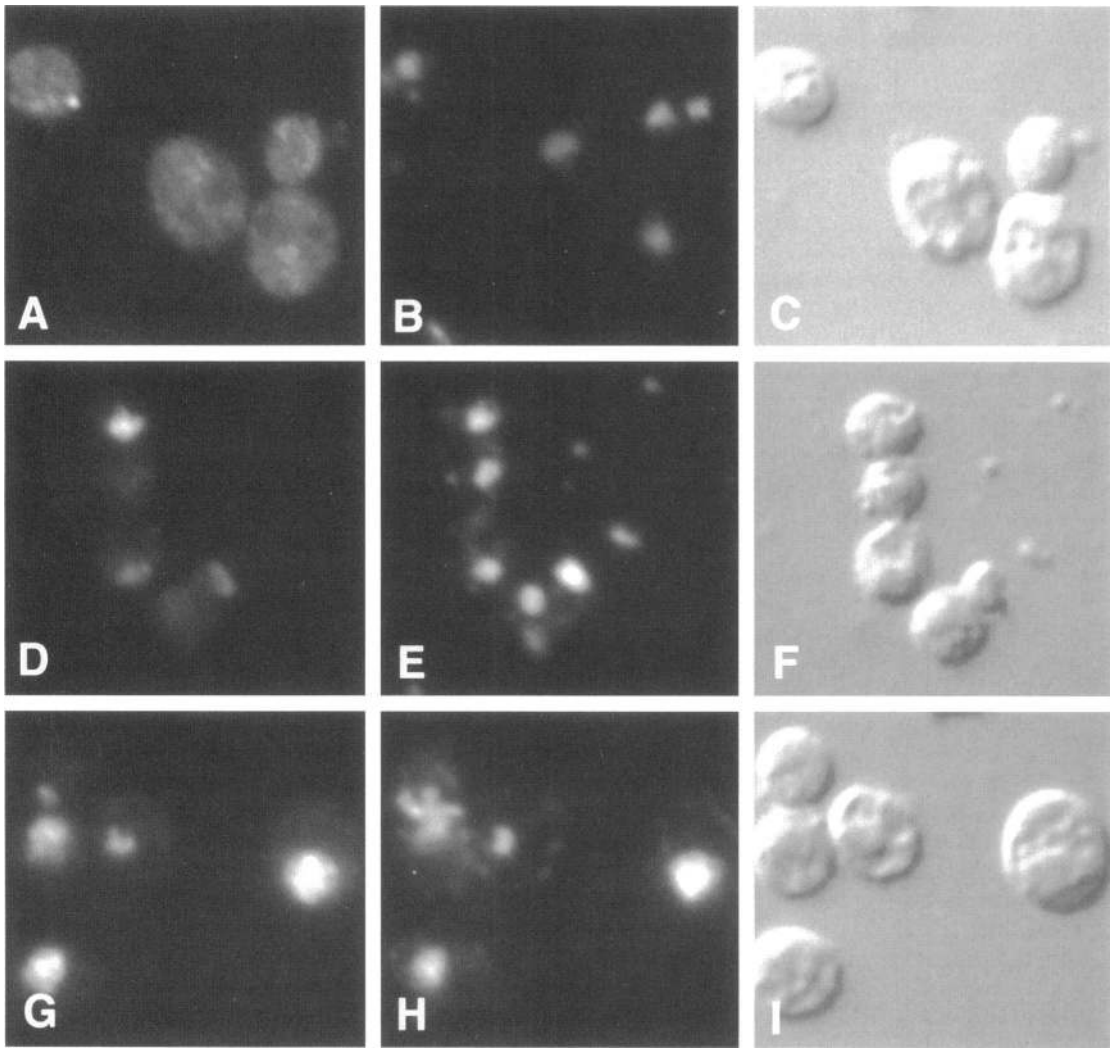

Figure 1. mRNA export is rapidly blocked when *rat9–1* cells are shifted to 37°C. The mRNA localization assay was performed on wild-type (FY23) or *rat9–1* cells (AGY401) grown continuously at 23°C or grown at 23°C and then shifted to 37°C for 1 h. The cells were counterstained with DAPI to visualize nuclei. (A) FITC fluorescence of wild-type cells grown at 37°C. (B) DAPI signal of cells in panel A. (C) DIC image of cells in panel A. (D) FITC fluorescence of *rat9–1* cells grown at 23°C. (E) DAPI signal of cells in panel D. (F) DIC image of cells in panel D. (G) FITC fluorescence of *rat9–1* cells shifted to 37°C. (H) DAPI signal of cells in panel G. (I) DIC image of cells in panel G. Identical exposure and printing conditions were used for panels A, D, and G.

from the cluster (see arrowheads). At this resolution, the pores always appeared to be embedded normally within the NE and did not appear to be detached from the pore membrane, as was reported for *nup145ΔN* (Wente and Blobel, 1994) The thin section in Figure 4E most likely represents an en face slice through the nucleus. In some sections, distortions of the NE were evident (Figure 4, C–F). Figure 4C shows a large projection of the NE reminiscent of abnormalities seen in cells with C-terminal truncations of *NUP1* (Bogerd *et al.*, 1994). Figure 4, D and F, shows nuclei where half of the perimeter of the NE appears as a single layer of NE while half consists of two layers of NE. Since these specimens were prepared to visualize the NPCs rather than the NE, it is not possible to be certain whether the NE is uninterrupted in the nuclei shown in Figure 4, D and F (see arrows). Of the 85 cells observed with near-medial sections through the nucleus, 15 had NE abnormalities similar to the cells in Figure 4, D and F, while the rest of the cells looked similar to the cell in Figure 4B.

Nucleolar fragmentation occurs in many strains containing mutant nucleoporins when mutant cells are shifted to nonpermissive temperatures (Kadowaki *et al.*, 1994a,b; Heath *et al.*, 1995). We examined the structure of the nucleolus in wild-type (FY23) and *rat9–1* strains (AGY401) by indirect immunofluorescence using either anti-Nsr1p mAb 2.3B, or anti-Nop1p mAb

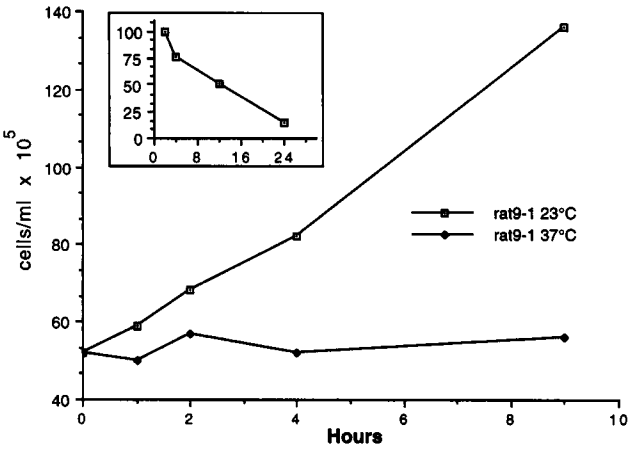

Figure 2. Growth and viability of *rat9–1* cells at 37°C. Aliquots removed from cultures of *rat9–1* cells (AGY401) grown continuously at 23°C or shifted to 37°C were fixed with formaldehyde immediately upon removal. Cells were counted in a hemacytometer. Each data point is the average of cell counts from three samples. Inset: to measure the loss of viability of *rat9–1* cells at 37°C, a culture of *rat9–1* cells grown continuously at 23°C was shifted to 37°C. Aliquots were removed and plated to YPD agar plates and incubated at 23°C. The x-axis represents the time in hours that the culture was incubated at 37°C. The y-axis represents the percentage of cells viable as determined by counting colonies on the YPD plates.

A66 (Aris and Blobel, 1988) to locate the nucleolus. Figure 5A shows the typical crescent-shaped staining pattern of nucleoli in wild-type cells shifted from 23°C to 37°C for 1 h. An identical staining pattern was seen in wild-type (our unpublished results) or *rat9–1* cells grown continuously at 23°C (Figure 5D). However, in *rat9–1* cells shifted from 23°C to 37°C for 1 h, two or more nucleolar fragments were clearly seen in nearly every nucleus (Figure 5G). The time course of nucleolar fragmentation was similar to that for accumulation of poly(A)$^+$ RNA, with nucleoli fragmenting within 15 min after the temperature shift to 37°C (our unpublished results).

Cloning and Sequencing of RAT9

We cloned the *RAT9* gene by complementation of the temperature-sensitive growth defect of strain AGY402 (*rat9–1*). Mutant cells were transformed with a wild-type centromeric genomic library marked with *URA3* (Rose *et al.*, 1987) and transformants selected on uracil drop-out media at 37°C. As the library was constructed in a shuttle plasmid, permitting replication in both yeast and *E. coli*, the plasmids were retrieved from six yeast colonies growing at 37°C and transformed into *E. coli*. Restriction endonuclease analysis of these plasmids, pRAT9.1 through pRAT9.6, showed that they were all related.

To physically map the complementing DNA, we probed an ordered set of yeast genomic lambda clones (Riles *et al.*, 1993). As a probe we used a 1.5-kbp *Dra*I fragment common to all the complementing clones. The probe hybridized to clones 1398 and 6607, which identify a locus on the right arm of chromosome X next to the *SSC1* gene. We also used the *Dra*I fragment to probe a blot of yeast chromosomes (Clonetech, Palo Alto, CA) and a Northern blot of yeast poly(A)$^+$ RNA. The probe hybridized to a chromosome band that contains both chromosomes XIV and X. The *Dra*I probe hybridized to an approximately 2.2-kb mRNA on the Northern blot (our unpublished results).

We subcloned a 5-kbp *Xba*I fragment from pRAT9.4, one of the original complementing plasmids that was able to complement the *rat9–1* mutation, and sequenced this DNA. This fragment contained three potential ORFs of 402, 480, and 2238 bp. We identified the 2238-bp ORF as *RAT9* by subsequent subcloning and mapping of the temperature-sensitive mutation (described below). Figure 6 shows the DNA sequence and the encoded protein, Rat9p. The ORF codes for a potential 84.9-kDa protein with an estimated pI = 4.30. Blast searches with *RAT9* and Rat9p did not identify any significant homologies in the databases (Altschul *et al.*, 1990). No distinguishing structural features are evident in Rat9p, although the protein contains three regions (amino acids 137–164, 424–456, and 691–716) predicted to have a 10–20% probability of forming coiled-coil interactions. The sequence of *RAT9/NUP85* has been registered with GenBank and has accession number U36469.

Isolation of the rat9–1 Allele

To formally prove that the 2238 ORF codes for the wild-type form of the gene mutated in the *rat9–1* allele, and to identify the mutation in *rat9–1*, we cloned the mutation of the *rat9–1* allele by gap-repair (see MATERIALS AND METHODS for details) (Rothstein, 1991). We discovered a C to A transversion at nucleotide 1287, which changes codon 404 from a serine (TCA) to a STOP (TAA). The stop codon truncates Rat9p from 744 to 404 amino acids.

We epitope tagged Rat9p with a fragment encoding three consecutive myc epitopes (EQKLISEEDLN). To determine whether the *rat9–1* allele is a null allele, we also epitope tagged the protein encoded by the mutant allele. The in-frame fusions between 3× myc and the wild-type and mutant alleles place the epitope tag three amino acids from the N-terminus of the proteins. The constructs were transformed into a *RAT9* deletion strain (described below) and whole-cell extracts were prepared for Western blot analysis. The Western blot was probed with the anti-myc antibody 9E10. The 9E10 antibody recognized an approximately 100-kDa protein in *RAT9* deletion cells bearing the pRAT9–25 plasmid ($RAT9_{myc}$), approximately 10 kDa larger than expected for the myc-tagged Rat9p protein (Figure 7,

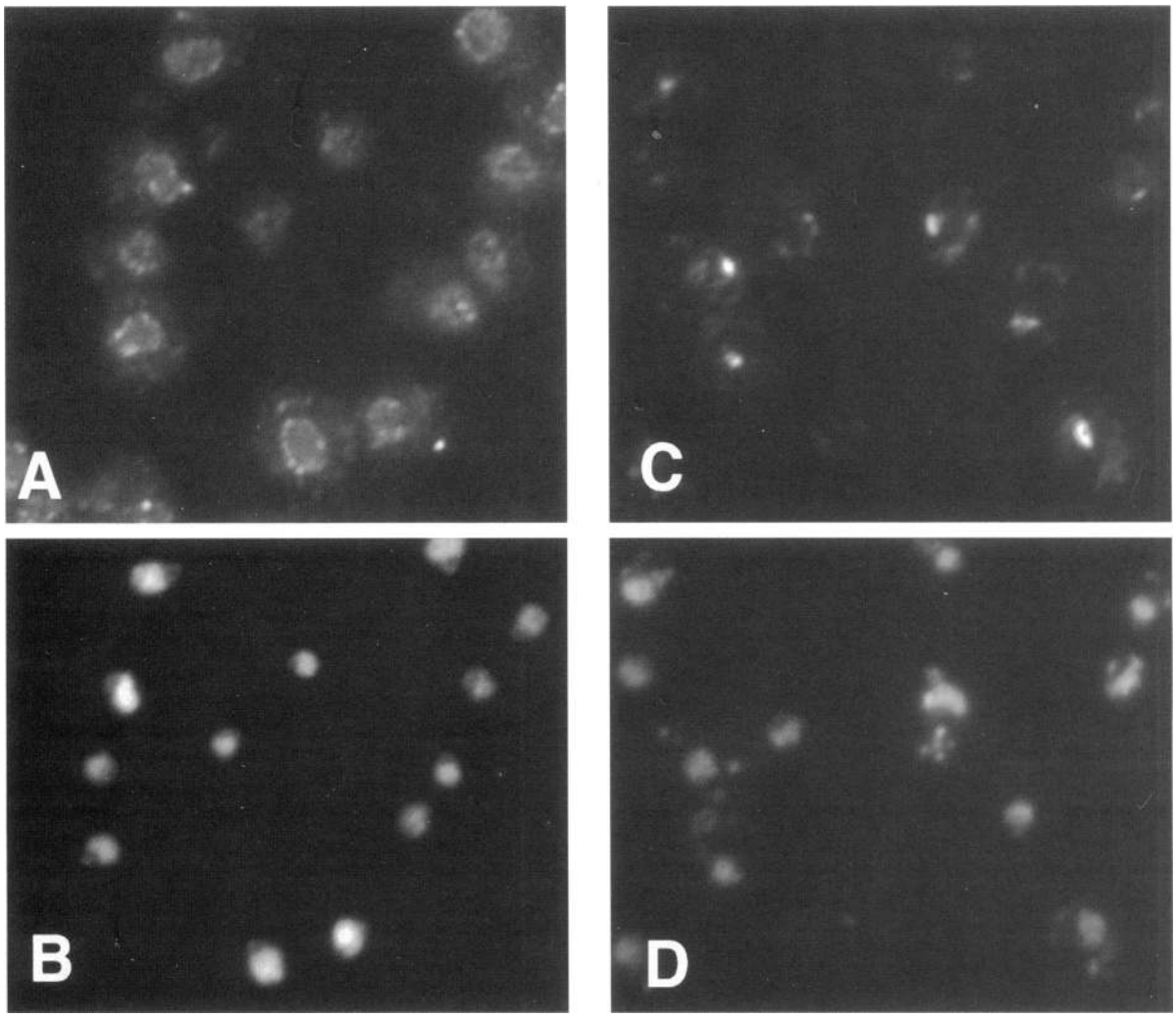

Figure 3. NPCs are clustered in *rat9–1* cells. Indirect immunofluorescence was performed on wild-type (FY23) or *rat9–1* cells (AGY401) grown continuously at 23°C, using antiserum raised against a GST-Rat7p/Nup159p fusion protein (Gorsch *et al.*, 1995). The cells were counterstained with Hoechst 33258 to visualize nuclei. (A) FITC fluorescence of wild-type cells. (B) Hoechst 33258 signal of cells in panel A. (C) FITC fluorescence of *rat9–1* cells. (D) Hoechst 33258 signal of cells in panel C.

lane 2). No protein was detected by the 9E10 antibody in either wild-type cells or *RAT9* deletion cells bearing the pRAT9–30 plasmid (*rat9–1*$_{myc}$) (Figure 7, lanes 1 and 3).

The entire *RAT9* gene was replaced with the *HIS3* auxotrophic marker to determine whether Rat9p is essential for vegetative growth (Baudin *et al.*, 1993). Haploid cells bearing either the original *rat9–1* allele or the deleted gene were able to grow equally well at 23°C without a plasmid-borne copy of *RAT9* but were unable to form colonies at 34°C or 37°C (Figure 8). Cells carrying the *rat9–1* mutation formed slightly larger colonies at 30°C than cells carrying a disruption of *RAT9*. *RAT9* deletion strains were examined for defects in mRNA export, NPC distribution, NE irregularities, and nucleolar integrity. To date we have not found any differences between the characteristics of *rat9–1* cells and the RAT9 deletion strain, other than the slight difference in growth properties at 30°C. We also examined the nuclear import of endogenous nuclear proteins (Npl3p, Nop1p, and Nsr1p) and a reporter protein (NLS_{H2B}-lacZ) in cells cultured continuously at 30°C, or shifted to 37°C for 2 h. We were unable to detect any mislocalization of these proteins

Figure 4 (facing page). Electron micrographs of wild-type (FY23), 37°C (A), and *rat9–1* (AGY195.204A), 23°C (B, C, and F); and 37°C (D and E) cells. Cells were grown continuously at 23°C and prepared as described in MATERIALS AND METHODS. Examples of isolated NPCs (white arrowheads), NPC clusters (black arrowheads), and possible discontinuities in the NE (black arrows). n, nucleus. Bar, 1 μm.

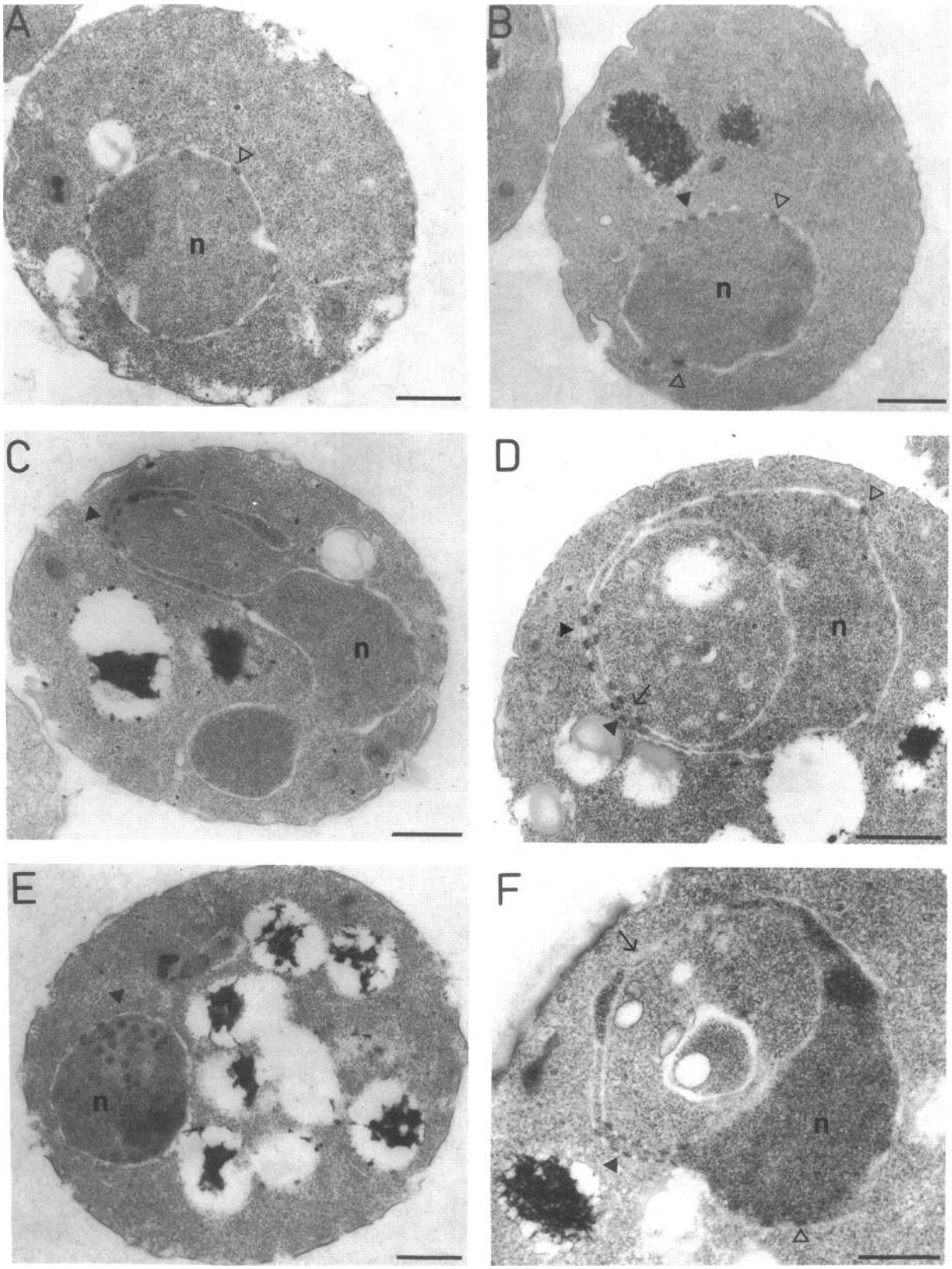

Figure 4 (cont).

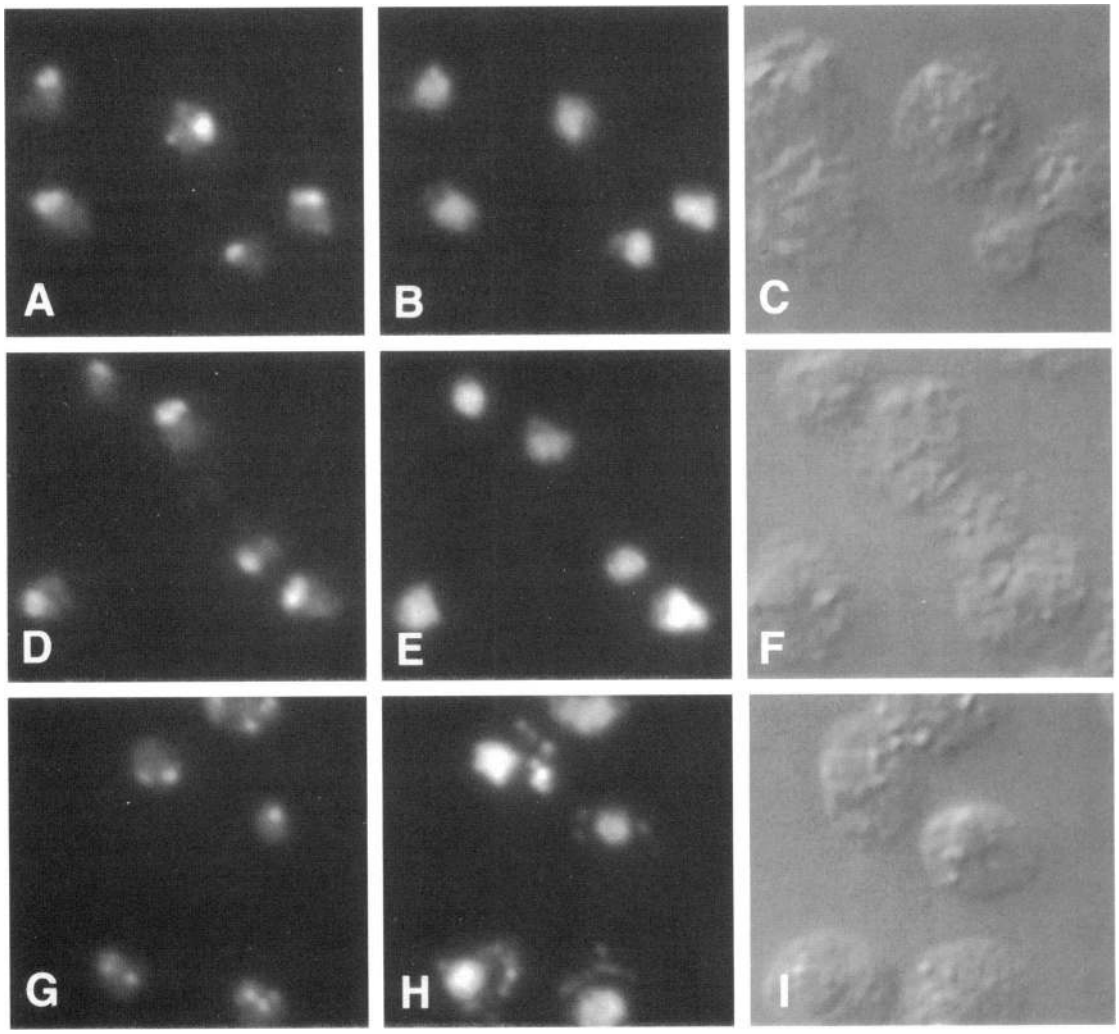

Figure 5. The nucleolus fragments when *rat9–1* cells are shifted to 37°C. Indirect immunofluorescence was done on wild-type (FY23) or *rat9–1* cells (AGY401) grown continuously at 23°C or grown at 23°C and then shifted to 37°C for 1 h. The cells were counterstained with Hoechst 33258 to visualize nuclei. (A) FITC fluorescence of wild-type cells grown at 37°C. (B) Hoechst 33258 signal of cells in panel A. (C) DIC image of cells in panel A. (D) FITC fluorescence of *rat9–1* cells grown at 23°C. (E) Hoechst 33258 signal of cells in panel D. (F) DIC image of cells in panel D. (G) FITC fluorescence of *rat9–1* cells grown at 37°C. (H) Hoechst 33258 signal of cells in panel G. (I) DIC image of cells in panel G.

in either *rat9–1* cells or cells carrying a disruption of *RAT9* (Goldstein, Snay and Cole, unpublished results).

Rat9p Co-localizes with NPC and Is Absent from the NPCs of rat2–1/nup120–1 Cells

We suspected that Rat9p might be localized to nuclear pores because clustered NPCs are often seen in cells with mutant nucleoporins (Copeland *et al.*, 1991; Wente and Blobel, 1993; Doye *et al.*, 1994; Gorsch *et al.*, 1995; Heath *et al.*, 1995; Li *et al.*, 1995). To determine the subcellular location of Rat9p, we epitope tagged it with GFP. GFP is a 26.9-kDa protein from the jellyfish *Aequorea victoria* that functions as an in vivo fluorescent molecular tag with spectral properties similar to FITC (Ward, 1979). An in-frame fusion between GFP and *RAT9* was constructed and transformed into a *RAT9* deletion strain. The RAT9 deletion strain with the RAT9-GFP construct was able to grow at 37°C, demonstrating that the fusion protein was functional. When cells bearing the RAT9-GFP construct were examined by either confocal microscopy (Figure 9A) or conventional fluorescence microscopy (Figure 9D), we observed punctate nuclear rim fluorescence as expected for a nucleoporin. To confirm that this fluorescence pattern represents NPC localization, the Rat9p-GFP cells were prepared for indirect immunofluorescence. NPCs were immunolocalized using antibodies against Rat7p/Nup159p (Gorsch *et al.*,

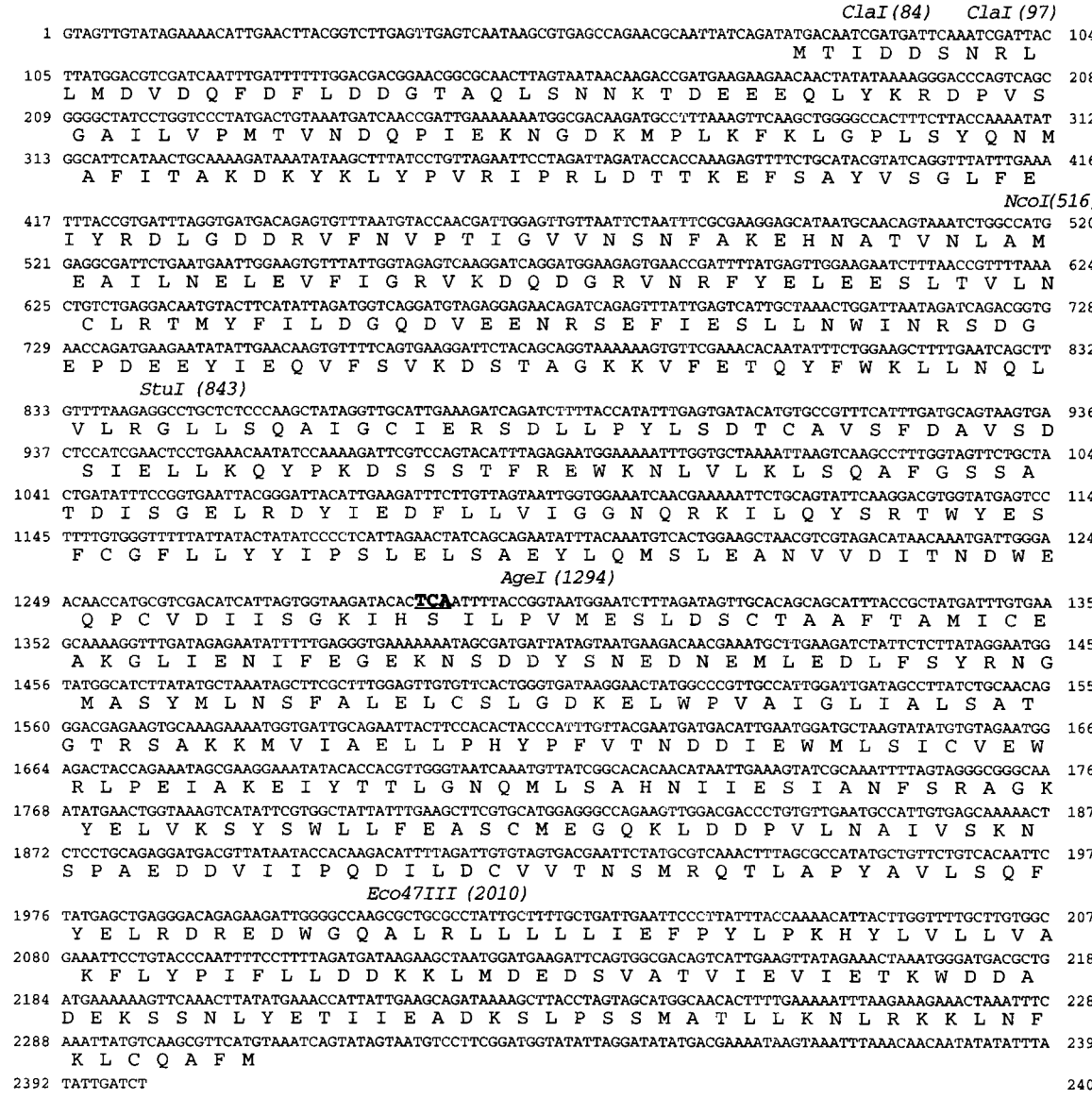

Figure 6. Nucleotide and predicted amino acid sequence of *RAT9/NUP85*. Nucleotides (2,400, including the 2,232 open reading frame) are shown. The bold-underlined TCA codon is mutated to the STOP codon TAA in the *rat9–1* allele. The restriction sites mark the location of the insertion of epitope tags (*Cla*I to *Cla*I) or sites used to generate gapped plasmids for gap-repair cloning of the *rat9–1* allele (*Cla*I, *Nco*I, *Stu*I, *Age* I, and *Eco47* III). The sequence is available from EMBL/GenBank/DDBJ under accession number U36469.

1995) as the primary antibody and a Texas Red-conjugated secondary antibody to visualize the location of Rat7p/Nup159p. We found that GFP fluoresced in fixed cells and co-localized with Rat7p/Nup159p (our unpublished results). Therefore, Rat9p is a nucleoporin, and we refer to it as Rat9p/Nup85p.

This result was also confirmed by conventional indirect immunofluorescence using the plasmid pRAT9.25 (Rat9p/Nup85p$_{myc}$) in a *RAT9* disruption strain (Figure 10). Rat9p/Nup85p$_{myc}$ was readily detected at the nuclear rim of wild-type cells (Figure 10A) and the pattern of staining was very similar to that observed using the RL-1 monoclonal antibody that recognizes yeast nucleoporins (Copeland and Snyder, 1993) (Figure 10D). Surprisingly, Rat9p/Nup85p$_{myc}$ could not be detected at the nuclear rim of *rat2–1/nup120–1* cells although RL-1 antigens were readily detected and were seen to be clustered at the nuclear rim as we reported previously (Figure 10I) (Heath *et al.*, 1995). We also examined whether Rat9p/Nup85p$_{myc}$ was localized to nuclear pores in cells carrying the *rat3–1/nup133–1* mutant allele. Rat9p/Nup85p$_{myc}$ was readily detected at nuclear pores (Figure 10K), in a clustered pattern very similar to that

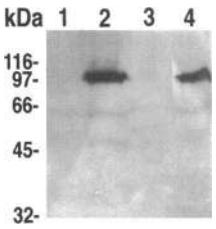

Figure 7. Western blot of Rat9p/Nup85p and rat9–1p. Logarithmically growing 23°C cultures were harvested and total cell lysates fractionated by SDS/PAGE. The blot was probed with anti-myc epitope (EQKLISEEDLN) mAb 9E10. Lane 1, FY23, wild type; lane 2, AGY909, *RAT9/NUP85* deletion with pRAT9.25 (Rat9p/Nup85p$_{myc}$); lane 3, AGY910, *RAT9/NUP85* deletion with pRAT9.30 (rat9–1p$_{myc}$); and lane 4, CHY110, *rat2–1/nup120–1* with pRAT9.25 (Rat9p/Nup85p$_{myc}$).

detected by the RL-1 antibody in these cells (Figure 10N). Rat9p/Nup85p$_{myc}$ was also present at NPCs in a *rat7–1/nup159–1* mutant strain (Heath and Cole, unpublished results). Thus, the absence of Rat9p/Nup85p$_{myc}$ from NPCs in *rat2–1/nup120–1* cells is specific because there was no difficulty detecting it at the nuclear rim in wild-type cells or in cells carrying mutant alleles of two other nucleoporins. These results provide evidence that Rat9p/Nup85p$_{myc}$ and Rat2p/Nup120p are part of a subcomplex of the NPC. We also examined the location of Rat9p/Nup85p-GFP in *rat2–1/nup120–1* cells transformed with plasmid pRAT9–28 (Rat9p/Nup85p$_{GFP}$) and saw fluorescence in vivo throughout the cell but without nuclear rim fluorescence (Figure 9B), confirming that Rat9p/Nup85p was absent from the NPCs in *rat2–1/nup120–1* cells.

Since it was possible that the reason we could not detect Rat9p/Nup85p-GFP or Rat9p/Nup85p$_{myc}$ at the nuclear rim in *rat2–1/nup120–1* cells was because the protein was absent or too inabundant, we prepared whole cell lysates of both *rat2–1/nup120–1* and wild-type cells carrying the plasmid encoding Rat9p/Nup85p$_{myc}$ and assayed the lysates by Western blotting. Using the 9E10 monoclonal antibody, we detected approximately the same level of Rat9p/Nup85p-$_{myc}$ in both of these strains (Figure 7, compare lanes 2 and 4). These data indicate that Rat9p/Nup85p was stable in *rat2–1/nup120–1* cells but did not appear to be incorporated into NPCs. Examination of panels A, F, and K in Figure 10 also shows that there was a higher level of cytoplasmic fluorescence in *rat2–1/nup120–1* cells than in wild-type or *rat3–1/nup133–1* cells, consistent with the protein being absent from NPCs but present in the cytoplasm of these cells. The cytoplasmic signal seen in wild-type and *rat3–1/nup133–1* cells probably results from overproduction of this protein, because centromere-based plasmids

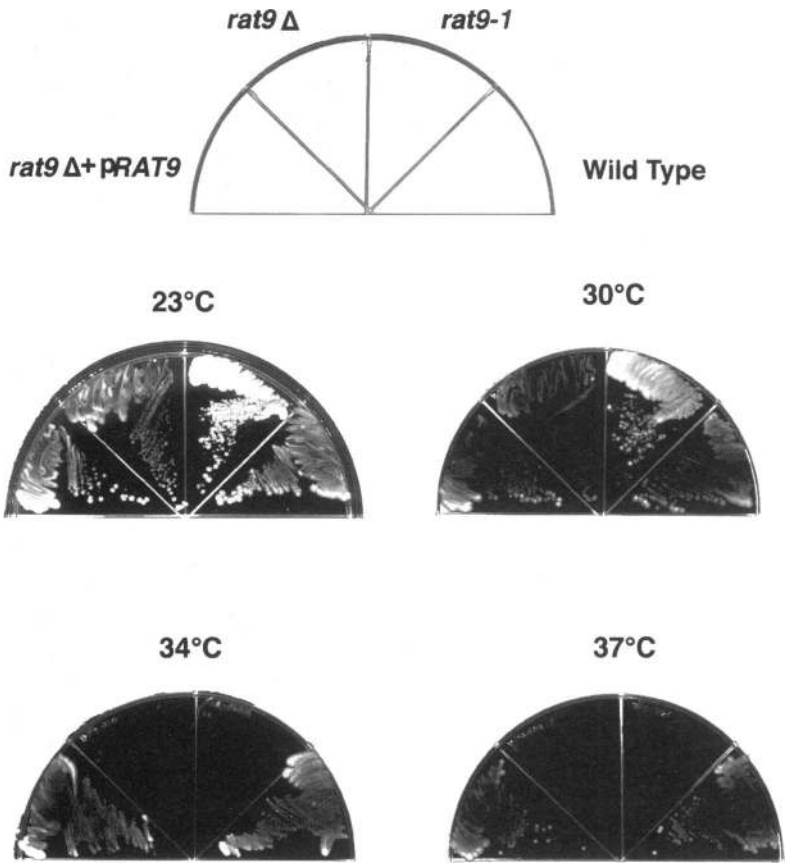

Figure 8. Growth properties of yeast strains bearing mutant alleles of *RAT9/NUP85*. All plates contained, from left to right, cells carrying a disruption of *RAT9/NUP85* and plasmid pRAT9 (CSY501), cells carrying a disruption of *RAT9/NUP85* (AGY917), cells carrying the *rat9–1* allele (AGY195.204A), or wild-type cells (FY23). All were plated onto YPD plates and incubated at 23°C, 30°C, 34°C, or 37°C for 5 days.

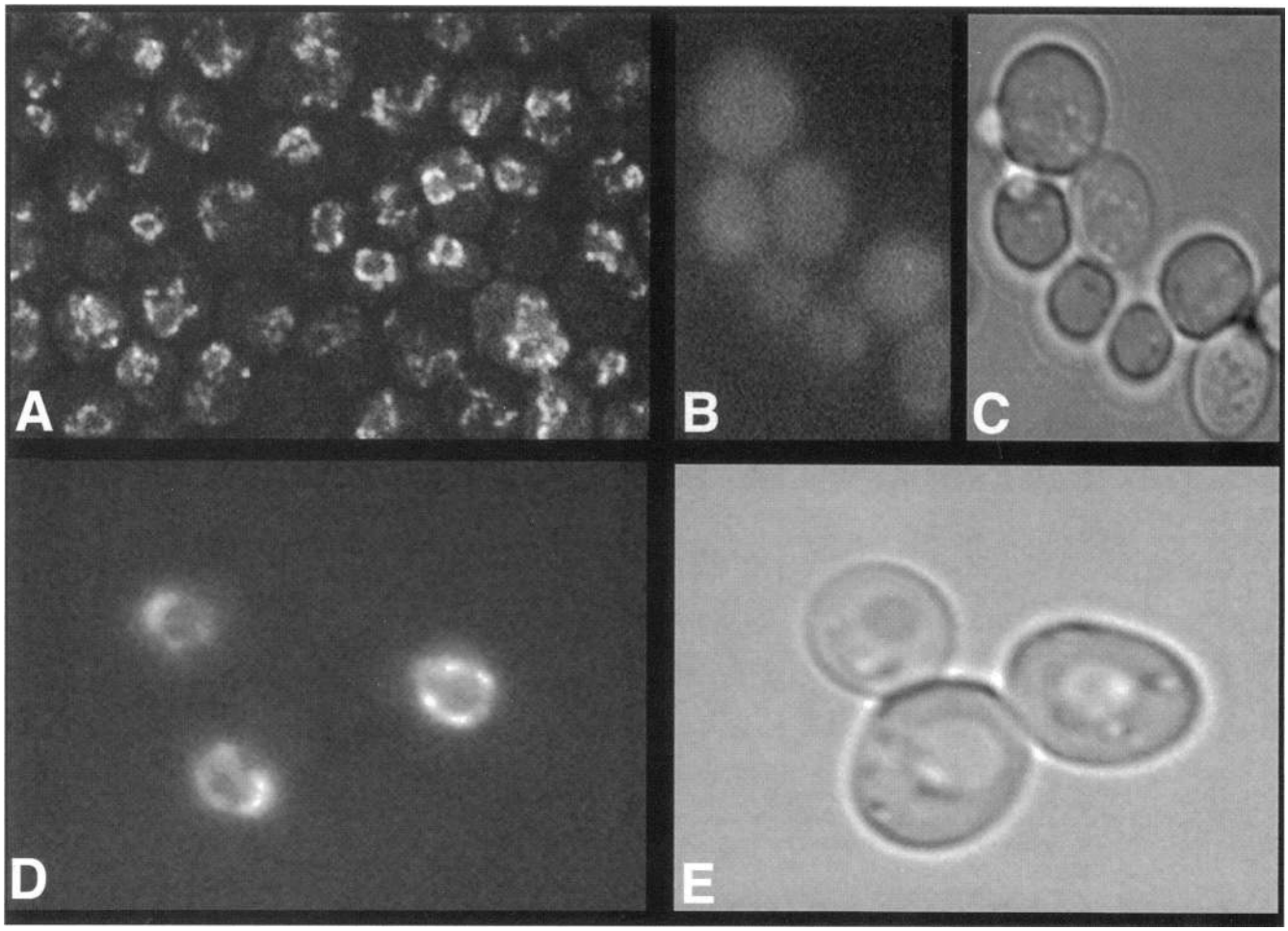

Figure 9. Rat9p/Nup85p is located at NPCs. *RAT9* deletion (AGY912) or *rat2–1/nup120–1* cells (AGY913) bearing a Rat9p/Nup85p-GFP (Green Fluorescent Protein) low copy plasmid were grown continuously at 23°C to mid-log phase. The cells were placed under coverslips and examined by either confocal microscopy (A) or fluorescence microscopy (B and D). (A and D) GFP fluorescence of a field of *rat9–1* cells showing typical punctate nuclear rim staining of NPCs. (B) GFP fluorescence of Rat9p/Nup85p-GFP in *rat2–1/nup120–1* cells. (C) DIC image of cells in panel B. (E) DIC image of cells in panel D. The exposure and printing times for panels B and D were identical.

are present in more than a single copy, and the chromosomal *RAT9/NUP85* locus is still present.

Synthetic Lethality

We tested whether mutations of *RAT9/NUP85* were synthetically lethal with mutations affecting other nucleoporins by mating haploid strains carrying mutant alleles of different nucleoporin genes. Heterozygous diploids were transformed with a centromere-based plasmid containing the wild-type *RAT9/NUP85* gene, sporulated, tetrads dissected, and analyzed as described in MATERIALS AND METHODS. We found that mutant alleles of *RAT9/NUP85* were synthetically lethal with a disruption of *RAT3/NUP133*, the *rat3–1/nup133–1* allele of *RAT3/NUP133*, a carboxy-terminal truncation of *NUP145*, and the *rat7–1* allele of *RAT7/NUP159*.

We wondered what the growth and RNA export behavior would be of a strain carrying mutant alleles of both *RAT9/NUP85* and *RAT2/NUP120*. We attempted to construct such a strain as part of a synthetic lethal analysis, but were unable to obtain sporulation of a strain heterozygous for mutations of *RAT9/NUP85* and *RAT2/NUP120*, regardless of whether it contained plasmid-borne copies of *RAT2/NUP120*, *RAT9/NUP85*, or neither. We were also unsuccessful in disrupting *RAT2/NUP120* in a haploid strain mutant for *RAT9/NUP85* or in disrupting *RAT9/NUP85* in a haploid strain mutant for *RAT2/NUP120*, regardless of whether or not the haploid contained a plasmid-borne copy of the disrupted gene. This suggests that mutations of *RAT2/NUP120* and *RAT9/NUP85* are synthetically lethal. This would not be surprising because there are only a few combinations of mutations

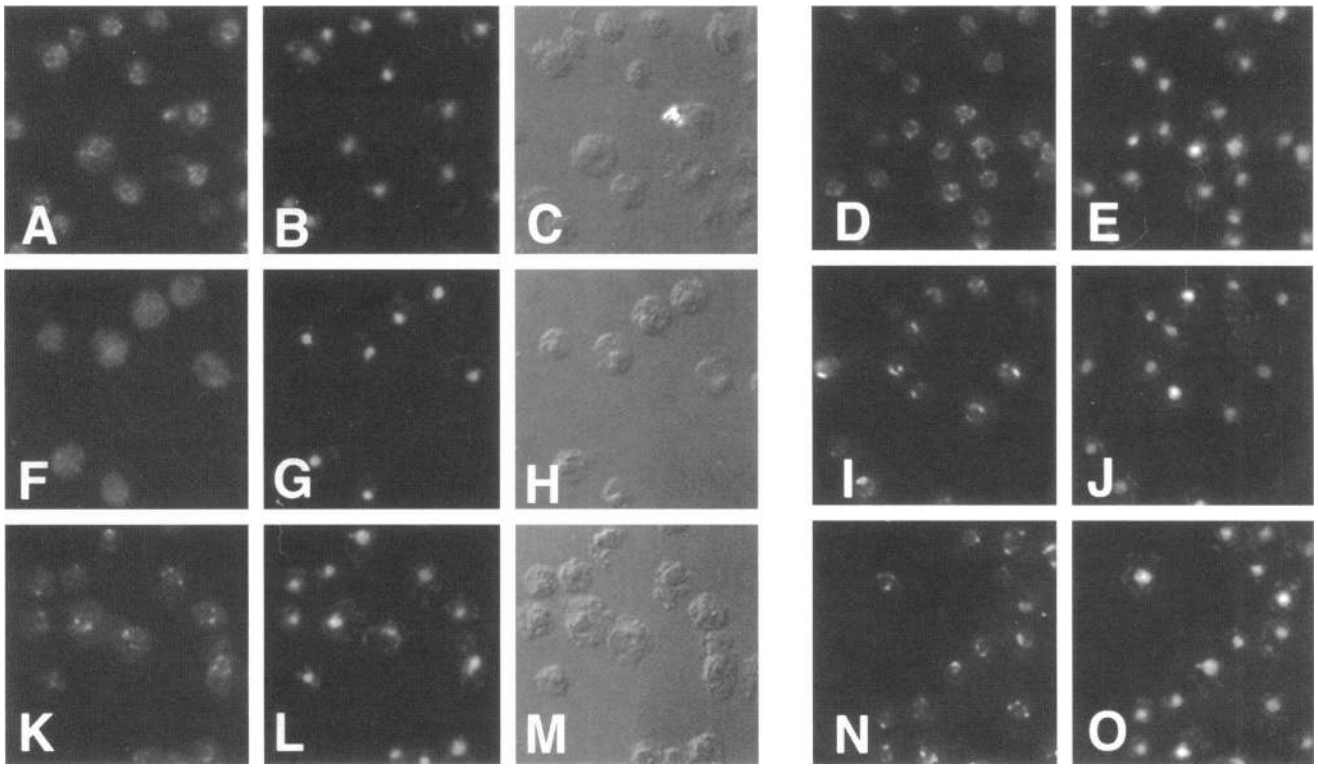

Figure 10. Absence of Rat9p/Nup85p from nuclear pores in *rat2–1/nup120–1* cells. Cells carrying a disruption of *RAT9*, or carrying the *rat2–1/nup120–1* or *rat3–1/nup133–1* mutant alleles were transformed with plasmid pRAT9.25 encoding the myc-tagged allele of Rat9p/Nup85p. Cells were grown continuously at 23°C to mid-log phase, fixed, and processed for indirect immunofluorescence microscopy using either monoclonal antibody 9E10 (to detect the myc epitope-tagged Rat9p/Nup85p) and a secondary goat anti-mouse antibody (against mouse IgG heavy chains) coupled to FITC or with monoclonal antibody RL1 (to detect the location of other yeast nucleoporins) and a secondary goat anti-mouse antibody (against IgM heavy chains) coupled to Texas Red. (A–E) Wild-type cells; (F–J) *rat2–1/nup120–1* mutant cells; and (K–O) *rat3–1/nup133–1* mutant cells. (A, F, and K) FITC fluorescence to detect Rat9p/Nup85p; (B, E, G, J, L, and O) DAPI staining to localize DNA; (C, H, and M) differential interference contrast microscopy of the fields of cells shown in panels B, G, and L, respectively; and (D, I, and N) Texas Red fluorescence to detect the location of other yeast nucleoporins.

to different nucleoporins that are not synthetically lethal out of approximately 100 pairs of mutations analyzed in various laboratories.

DISCUSSION

In a screen for mRNA export mutants we identified Rat9p/Nup85p, a novel *S. cerevisiae* nucleoporin. *RAT9* deletion strains or *rat9–1* cells have variable amounts of poly(A)$^+$ RNA trapped in their nuclei at 23°C but nearly 100% of the cells cease exporting mRNA within 15 min after being shifted to 37°C. After a 1-h shift to 37°C, the cytoplasm of mutant cells was dark. Although it is possible that in *rat9–1* cells there is increased turnover of cytoplasmic mRNA creating an apparent accumulation of mRNA in the nucleus, this seems very unlikely given the even fluorescent staining pattern of wild-type cells (Figure 1), the striking and bright fluorescent signal in nuclei of *rat9–1* cells shifted to 37°C (Figure 1), and the location of Rat9p/Nup85p at the nuclear pore.

Several lines of evidence point to Rat9p/Nup85p being a nucleoporin. Constitutive NPC clustering is a common defect for several mutant nucleoporins. NPC clustering was reported previously for both temperature-sensitive and disruption strains of *RAT2/NUP120* or *RAT3/NUP133* (Doye *et al.*, 1994; Heath *et al.*, 1995; Li *et al.*, 1995) and in a disruption of the amino-terminal half of Nup145p (Wente and Blobel, 1994). A temperature-sensitive allele of *RAT7/NUP159* results in NPC clustering at the permissive temperature but a more normal distribution of NPCs is seen when mutant cells are shifted to the nonpermissive temperature (Gorsch *et al.*, 1995). We epitope-tagged Rat9p/Nup85p with the in vivo molecular marker GFP, and separately with a triple "myc" epitope tag. Deletion strains carrying a *RAT9/NUP85-GFP* plasmid fluoresced in the typical punctate nuclear rim staining pattern diagnostic of NPCs. We also co-localized

Rat9p/Nup85p-GFP with Rat7p/Nup159p by indirect immunofluorescence. Similar findings were obtained using myc-tagged Rat9p/Nup85p. Finally, synthetic lethality was observed between mutant alleles of *RAT9/NUP85* and mutant alleles of several other nucleoporins.

Abnormalities of the NE in rat9 Mutant Cells

The most visually striking defects found in *rat9–1* cells are the abnormalities of the NE. A defect in NE integrity is a common phenotype of some strains carrying mutant alleles of yeast nucleoporins. Interestingly, different mutant strains have distinct phenotypes. Deletion of *NUP116* results in herniations of the outer nuclear membrane so that a seal is formed over the NPCs in cells shifted to the nonpermissive temperature of 37°C (Wente and Blobel, 1993). The sealed NPCs appear to remain export competent as judged by the accumulation of electron dense material within the herniations but on the cytoplasmic side of the NPC. *nup116Δ* cells also have long thin invaginations of the inner NE extending into the nucleoplasm. These phenotypes suggest that Nup116p could act as a rivet between the NPC and the pore membrane (Wente and Blobel, 1993). Deletion/disruptions of the N-terminus of Nup145p result in the formation of successive and interconnected herniations of the NE that enclose clusters of NPCs (Wente and Blobel, 1994). These "grape-like" clusters of NPCs were frequently found under a protrusion of the outer nuclear membrane. In contrast to *nup116Δ* cells, *nup145ΔN* cells appear to be fully competent for RNA export as judged by their near wild-type growth rate at temperatures between 17°C and 37°C. Here again, as with *nup116Δ*, it seems as if at least one function of Nup145p is to secure the NPC to the pore membrane, albeit in a way different from Nup116p. Carboxy-terminal truncations of Nup1p result in temperature-sensitive growth, defects in nuclear migration, randomly oriented mitotic spindles, and long projections of NE extending into the cytoplasm (Bogerd *et al.*, 1994). Bogerd and colleagues proposed a role for Nup1p in maintaining structural integrity of the NE by connecting the NPC to the underlying nucleoskeleton. They hypothesized that this connection was required to allow the proper orientation of the nucleus by responding to cytoskeletal forces transmitted through the spindle pole body.

In thin-section electron micrographs of *rat9–1* cells, we frequently observed what appeared to be long protrusions of NE emanating from the main body of the nucleus. We can interpret this striking configuration of the NE, shown in Figure 4, D and F, in two ways. If part of the NE is invaginated, a thin section viewed perpendicular to the invagination would look like Figure 4, D and F. A similar geometry could be achieved if two projections of NE were pulled away from the main body of the nucleus such that the tips of the projections were closely apposed or fused. The projections could either be finger like or similar to a pair of cupped hands.

The NE abnormalities of *rat9–1* cells are most like those found in the carboxy-terminal truncation mutants of Nup1p. In the cases of *nup116Δ* and *nup145ΔN*, one of the nuclear membranes seems to have lost continuity with the main body of the nucleus while in *nup1* and *rat9/nup85* mutants, both nuclear membranes have lost this continuity. This suggests that while Nup116p and Nup145p could have roles in tethering NPCs to the pore membrane, Nup1p and Rat9p/Nup85p are more likely to have functions connecting the NE to either the cytoskeleton or nucleoskeleton. Unlike Nup1p mutants, Rat9p/Nup85p mutants do not appear to have defects in nuclear segregation during mitosis (Figure 1, E and F) or in nuclear protein import. This suggests that although Nup1p and Rat9p/Nup85p may have some similar functions, they also have distinct ones.

Constitutive NPC clustering is a common defect found in many strains containing a mutant nucleoporin. In addition to nup116Δ, nup145ΔN, and carboxy deletions of Nup1p, both mutation or deletion of *RAT3/NUP133* or *RAT2/NUP120* result in clustered NPCs (Doye *et al.*, 1994; Heath *et al.*, 1995; Li *et al.*, 1995). However, unlike the four nucleoporins discussed above, perturbations of the NE were not seen in strains carrying null alleles of *RAT2/NUP120* or *RAT3/NUP133*. It is likely that there are several different mechanisms for NPCs to become clustered. NPC clustering could reflect a defect in the proper distribution of NPCs. For example, if NPCs are normally inserted into or assembled within the NE at a single site, then a failure to disperse normally would result in NPC clustering. Such failure might be the result of opportunistic protein-protein interactions that occur when a nucleoporin or NPC subcomplex is missing. In the cases of *nup1* mutants and *rat9–1* it seems quite possible that the clustering of NPCs follows from specific NE defects. In these mutants, NPCs are brought into close apposition with one another in adjacent sheets of NE. Perhaps the nucleoplasmic elements of opposing NPCs interact to lock pairs of NPCs together. Notice that in Figure 4, C–E, the clustered NPCs often appear to be in register between opposing sheets of NE.

Fragmentation of the Nucleolus in rat9 Mutant Cells

Among the pleiotropic defects observed in *rat9–1* cells is fragmentation of the nucleolus when the cells were

shifted to the nonpermissive temperature. This phenotype has been seen previously in yeast strains carrying temperature-sensitive alleles of other nucleoporins or of RNA polymerase I (Oakes *et al.*, 1993; Kadowaki *et al.*, 1994a,b). Heat shock also causes fragmentation of the nucleolus (Simard and Bernhard, 1967). Under conditions where nucleolar fragmentation was observed, co-localization of poly(A)$^+$ RNA and nucleolar antigens has also been observed (Kadowaki *et al.*, 1995). These and other data have led to the hypothesis that the nucleolus has a normal role in mRNA maturation and/or export (Sidebottom and Harris, 1969; Schneiter *et al.*, 1995). Although the mRNA export block and nucleolar fragmentation are coincident after shifting *rat9–1* cells to 37°C, we have no evidence to show that the mRNA export block is a result of nucleolar fragmentation. Perhaps the abnormal accumulation of poly(A)$^+$ RNA (and other RNAs) in nuclei defective for RNA export perturbs overall nuclear structure, resulting in nucleolar fragmentation. In support of this idea, we have found that rRNA synthesis is completely inhibited within 15 min of a shift to 37°C in yeast strains bearing temperature-sensitive alleles of *RAT10/NUP145* and *RAT7/NUP159* (Dockendorff, Del Priore, and Cole, unpublished results). Fragmentation of the nucleolus appears also to be a direct result of cessation of rRNA synthesis and ribosome biogenesis in strains with temperature-sensitive alleles of RNA polymerase I (Oakes *et al.*, 1993), and co-localization of poly(A)$^+$ RNA and nucleolar antigens was also seen in this mutant strain. Perhaps fragmentation of the nucleolus permits nucleolar RNA binding proteins to interact with poly(A)$^+$ RNA. Such interactions might normally be prevented by nucleolar architecture sequestering these proteins in regions of the nucleolus normally inaccessible to poly(A)$^+$ RNA.

Evidence for an NPC Subcomplex Containing Rat9p/Nup85p and Rat2p/Nup120p that Is Important for RNA Export

We found that Rat9p/Nup85p could not be detected in NPCs of cells bearing a temperature-sensitive allele of *RAT2/NUP120* but was readily detected in NPCs in strains bearing mutant alleles of *RAT3/NUP133* and *RAT7/NUP159*. This conclusion is based upon our inability to visualize Rat9p/Nup85p tagged with either GFP or the myc epitope in *rat2–1/nup120–1* cells and the presence of Rat9p/Nup85p-$_{myc}$ (Figure 7) and Rat9p/Nup85p-GFP (Goldstein, Snay, and Cole, unpublished results) in extracts of these cells. Since the absence of Rat9p/Nup85p from NPCs occurs in *rat2–1/nup120–1* cells growing continuously at the permissive temperature of 23°C, we think it likely that the NPCs produced in *rat2–1/nup120–1* cells lack Rat9p/Nup85p, but it is also possible that Rat9p/Nup85p is assembled into NPCs under these conditions but is anchored within the NPC sufficiently weakly so that it is rapidly lost. The dependence on Rat2p/Nup120p for Rat9p/Nup85p to be in NPCs suggests that the two are components of an NPC subcomplex. To address this latter possibility, we attempted to co-immunoprecipitate these proteins from a yeast strain containing either GFP-tagged Rat9p/Nup85p or myc-tagged Rat2p/Nup120p. Unfortunately the background from the rabbit polyclonal anti-GFP antiserum was too high and the efficiency of immunoprecipitation with the anti-myc antibody 9E10 too low to answer this question.

How directly involved in mRNA export is Rat9p/Nup85p? NPC clustering and abnormalities of the NE are common phenotypes in several strains carrying mutant alleles of nucleoporins. This suggests that proper distribution of NPCs and their proper interaction with the NE or nucleoskeleton are readily perturbed by mutation of individual nucleoporins. It is probable that most nucleoporins are components of NPC subassemblies, and therefore an entire subassembly may be defective (or absent) if a single nucleoporin is mutant or absent. The integrity of most NPC subassemblies may be required for proper NPC distribution and interaction of NPCs with the NE, the nucleoskeleton, and the cytoskeleton. On the other hand, rapid accumulation of poly(A)$^+$ RNA (accumulation in 100% of cells within 1 h of a shift to 37°C) has been seen in only a small subset of strains carrying disruptions or mutant alleles of nucleoporin genes. These include strains with mutations of *RAT7/NUP159* (Gorsch *et al.*, 1995; Kraemer *et al.*, 1995), *NUP145* (Fabre, 1994; Dockendorff, Goldstein, and Cole, unpublished results), *NUP82* (Grandi *et al.*, 1995; Hurwitz and Blobel, 1995), and *RAT9/NUP85*. In strains with mutations of *RAT2/NUP120* (Aitchison *et al.*, 1995; Heath *et al.*, 1995) or *RAT3/NUP133* (Doye *et al.*, 1994; Li *et al.*, 1995) approximately 3–4 h are required for maximum accumulation of poly(A)$^+$ RNA in the nuclei of cells shifted to 37°C. In yeast strains carrying mutant alleles of other nucleoporin genes, the mutations appear to affect protein import to a much greater degree than they affect RNA export (e.g. *NUP1*; Bogerd *et al.*, 1994). This suggests that specific nucleoporins, or perhaps entire subassemblies, are specialized for roles in protein import or RNA export. The rapid accumulation of poly(A)$^+$ RNA in strains carrying mutant alleles of *RAT9/NUP85*, combined with the lack of a detectable nuclear protein import defect, suggest that Rat9p/Nup85p is a component of a subassembly of the NPC involved in RNA export.

How can we explain the rapid nuclear accumulation of poly(A)$^+$ RNA in cells carrying the *rat9–1* allele or a null allele of *RAT9/NUP85* and its much slower accumulation in cells carrying the *rat2–1/nup120–1* allele or a disruption of *RAT2/NUP120*? This suggests that cells lacking Rat2p/Nup120p are less defective

for RNA export than are cells with a null allele of *RAT9/NUP85*. However, the NPCs in cells lacking Rat2p/Nup120p appear to lack Rat9p/Nup85p. We can imagine several possible explanations. Although the NPCs from cells carrying a disruption or other mutation of *RAT2/NUP120* do not appear to contain Rat9p/Nup85p, perhaps Rat2p/Nup120p and Rat9p/Nup85p are the only proteins missing from NPCs in these cells, while the NPCs in cells mutant for *RAT9/NUP85* may also lack other nucleoporins. This is consistent with the recent finding that Rat9p/Nup85p and Rat2p/Nup120p are components of a subcomplex also containing Nup84p, Seh1p, and a low level of Sec13p (Siniossoglou, *et al.*, 1996). Another possibility is that Rat9p/Nup85p can perform some of its functions even when it does not associate with the NPC or associates only transiently. Alternatively, perhaps NPCs in *RAT2/NUP120* null cells retain a low level of Rat9p/Nup85p that is not detectable by immunofluorescence. More extensive studies will be required to develop a picture of the degree to which various nucleoporins require specific other nucleoporins for their incorporation into or retention within the NPC.

ACKNOWLEDGMENTS

We thank John Aris, Mike Snyder, and Larry Gerace for antibodies and Mike Moser for the GFP plasmid. We also thank Pamela Silver and Gerry Fink for plasmids and Mark Rose for the *URA3 CEN* library. We especially thank Louisa Howard, Ann Lavanway, and Ken Orndorff for expert assistance with microscopy. We thank the members of our lab, especially Veronica del Priore, for critically reading this manuscript. These studies were supported by National Institutes of Health grant GM-33998 to C.N.C. and by a National Cancer Institute core grant (CA-16038) to the Norris Cotton Cancer Center. A.L.G. was supported by NIH training grant CA-09658.

REFERENCES

Aitchison, J.D., Blobel, G., and Rout, M.P. (1995). Nup120p: a yeast nucleoporin required for NPC distribution and mRNA transport. J. Cell Biol. *131*, 1659–1675.

Altschul, S.F., Gish, W., Miller, W., Myers, E.W., and Lipman, D.J. (1990). Basic local alignment search tool. J. Mol. Biol. *215*, 403–410.

Amberg, D.C., Goldstein, A.L., and Cole, C.N. (1992). Isolation and characterization of RAT1: an essential gene of *Saccharomyces cerevisiae* required for the efficient nucleocytoplasmic trafficking of mRNA. Genes Dev. *6*, 1173–1189.

Aris, J.P., and Blobel, G. (1988). Identification and characterization of a yeast nucleolar protein that is similar to a rat liver nucleolar protein. J. Cell Biol. *107*, 17–31.

Baudin, A., Ozier-Kalogeropoulos, O., Denouel, A., Lacroute, F., and Cullin, C. (1993). A simple and efficient method for direct gene deletion in *Saccharomyces cerevisiae*. Nucleic Acids Res. *21*, 3329–3330.

Boeke, J.D., Trueheart, J., Natsoulis, G., and Fink, G.R. (1987). 5-fluoro-orotic acid as a selective agent in yeast molecular genetics. Methods Enzymol. *154*, 164–175.

Bogerd, A.M., Hoffman, J.A., Amberg, D.C., Fink, G.R., and Davis, L.I. (1994). *nup1* mutants exhibit pleiotropic defects in nuclear pore complex function. J. Cell Biol. *127*, 319–332.

Byers, B., and Goetsch, L. (1975). Behavior of spindles and spindle plaques in the cell cycle and conjugation of *Saccharomyces cerevisiae*. J. Bacteriol. *124*, 511–523.

Copeland, C.S., Amberg, D.C., and Cole, C.N. (1991). Clustering of nuclear pore complexes in mRNA trafficking mutants of *Saccharomyces cerevisiae*. J. Cell Biol. *115*, 317a.

Copeland, C.S., and Snyder, M. (1993). Nuclear pore complex antigens delineate nuclear envelope dynamics in vegetative and conjugating *Saccharomyces cerevisiae*. Yeast *9*, 235–249.

Doye, V., Wepf, R., and Hurt, E.C. (1994). A novel nuclear pore protein Nup133p with distinct roles in poly(A)$^+$ RNA transport and nuclear pore distribution. EMBO J. *13*, 6062–6075.

Dworetzky, S.I., and Feldherr, C.M. (1988). Translocation of RNA-coated gold particles through the nuclear pores of oocytes. J. Cell. Biol. *106*, 575–584.

Fabre, E., Boelens, W.C., Wimmer, C., Mattaj, I.W., and Hurt, E.C. (1994). Nup145p is required for nuclear export of mRNA and binds homopolymeric RNA in vitro via a novel conserved motif. Cell *78*, 275–289.

Feldherr, C.M., Kallenbach, E., and Schultz, N. (1984). Movement of a karyophilic protein through the nuclear pore complex. J. Cell Biol. *99*, 2216–2222.

Forbes, D.J. (1992). Structure and function of the nuclear pore complex. Annu. Rev. Cell Biol. *8*, 495–527.

Gietz, R.D., and Sugino, A. (1988). New yeast-*Escherichia coli* shuttle vectors constructed with in vitro–mutagenized yeast genes lacking six-base pair restriction sites. Gene *74*, 527–534.

Gorsch, L.C., Dockendorff, T.C., and Cole, C.N. (1995). A conditional allele of the novel repeat-containing yeast nucleoporin *RAT7/NUP159* causes both rapid cessation of mRNA export and reversible clustering of nuclear pore complexes. J. Cell Biol. *129*, 939–955.

Grandi, P., Emig, S., Weise, C., Hucho, F., Pohl, T., and Hurt, E.C. (1995). A novel nuclear pore protein Nup82p which specifically binds to a fraction of Nsp1p. J. Cell Biol. *130*, 1263–1273.

Guthrie, C., and Fink, G.R. (1991). Guide to yeast genetics and molecular biology. Methods Enzymol. *194*, 423–424.

Heath, C.V., Copeland, C.S., Amberg, D.C., Del Priore, V., Snyder, M., and Cole, C.N. (1995). Nuclear pore complex clustering and nuclear accumulation of poly(A)$^+$ RNA associated with mutation of the *Saccharomyces cerevisiae RAT2/NUP120* gene. J. Cell Biol *131*, 1677–1697.

Heim, R., Cubitt, A.B., and Tsien, R.Y. (1995). Improved green fluorescence. Nature *373*, 663–664.

Hurwitz, M.E., and Blobel, G. (1995). NUP82 is an essential yeast nucleoporin required for poly(A)$^+$ RNA export. J. Cell Biol. *130*, 1275–1281.

Kadowaki, T., Chen, S., Hitomi, M., Jacobs, E., Kumagai, C., Liang, S., Schneiter, R., Singleton, D., Wisniewska, J., and Tartakoff, A.M. (1994a). Isolation and characterization of *Saccharomyces cerevisiae* mRNA transport-defective (mtr) mutants. J. Cell Biol. *126*, 649–659.

Kadowaki, T., Hitomi, M., Chen, S., and Tartakoff, A.M. (1994b). Nuclear mRNA accumulation causes nucleolar fragmentation in yeast *mtr2* mutant. Mol. Biol. Cell *5*, 1253–1263.

Kadowaki, T., Schneiter, R., Hitomi, M., and Tartakoff, A.M. (1995). Mutations in nucleolar proteins lead to nucleolar accumulation of PolyA+ RNA in *Saccharomyces cerevisiae*. Mol. Biol. Cell *6*, 1103–1110.

Kraemer, D.M., Strambio-de-Castillia, C., Blobel, G., and Rout, M.P. (1995). The essential yeast nucleoporin NUP159 is located on the cytoplasmic side of the nuclear pore complex and serves in karyopherin-mediated binding of transport substrate. J. Biol. Chem. *270*, 19017–19021.

Li, O., Heath, C.V., Amberg, D.C., Dockendorff, T.C., Copeland, C.S., Snyder, M., and Cole, C.N. (1995). Mutation or deletion of the *Saccharomyces cerevisiae RAT3/NUP133* gene causes temperature-dependent nuclear accumulation of poly(A)$^+$ RNA and constitutive clustering of nuclear pore complexes. Mol. Biol. Cell *6*, 401–417.

Melchior, F., Paschal, B., Evans, J., and Gerace, L. (1993). Inhibition of nuclear protein import by nonhydrolyzable analogues of GTP and identification of the small GTPase Ran/TC4 as an essential transport factor. J. Cell Biol. *123*, 1649–1659.

Mirzayan, C., Copeland, C.S., and Snyder, M. (1992). The NUF1 gene encodes an essential coiled-coil related protein that is a potential component of the yeast nucleoskeleton. J. Cell Biol. *116*, 1319–1332.

Moore, M.S., and Blobel, G. (1993). The GTP-binding protein Ran/TC4 is required for protein import into the nucleus. Nature *365*, 661–663.

Moroianu, J., and Blobel, G. (1995). Protein export from the nucleus requires the GTPase Ran and GTP hydrolysis. Proc. Natl. Acad. Sci. USA *92*, 4318–4322.

Oakes, M., Nogi, Y., Clark, M.W., and Nomura, M. (1993). Structural alterations of the nucleolus in mutants of *Saccharomyces cerevisiae* defective in RNA polymerase I. Mol. Cell. Biol. *13*, 2441–2455.

Radu, A., Moore, M.S., and Blobel, G. (1995). The peptide repeat domain of nucleoporin Nup98 functions as a docking site in transport across the nuclear pore complex. Cell *81*, 215–222.

Reichelt, R., Holzenburg, A., Buhle, E.L., Jr., Jarnik, M., Engel, A., and Aebi, U. (1990). Correlation between structure and mass distribution of the nuclear pore complex and of distinct pore complex components. J. Cell. Biol. *110*, 883–894.

Riles, L., Dutchik, J.E., Baktha, A., McCauley, B.K., Thayer, E.C., Leckie, M.P., Braden, V.V., Depke, J.E., and Olson, M.V. (1993). Physical maps of the six smallest chromosomes of *Saccharomyces cerevisiae* at a resolution of 2.6 kilobase pairs. Genetics *134*, 81–150.

Rosbash, M., and Singer, R.H. (1993). RNA travel: tracks from DNA to the cytoplasm. Cell *75*, 399–401.

Rose, M.D., Novick, P., Thomas, J.H., Botstein, D., and Fink, G.R. (1987). A *Saccharomyces cerevisiae* genomic plasmid bank based on a centromere-containing shuttle vector. Gene *60*, 237–243.

Rose, M.D., Winston, F., and Hieter, P. (1989). Methods In Yeast Genetics, Cold Spring Harbor, NY: Cold Spring Harbor Laboratory Press.

Rothstein, R. (1991). Targeting, disruption, replacement, and allele rescue: integrative DNA transformation in yeast. Methods Enzymol. *194*, 281–301.

Rout, M.P., and Blobel, G. (1993). Isolation of the yeast nuclear pore complex. J. Cell Biol. *123*, 771–783.

Rout, M.P., and Wente, S.R. (1994). Pores for thought: nuclear pore complex proteins. Trends Cell Biol. *4*, 357–365.

Schneiter, R., Kadowaki, T., and Tartakoff, A.M. (1995). mRNA transport in yeast: time to reinvestigate the functions of the nucleolus. Mol. Biol. Cell *6*, 357–370.

Sidebottom, E., and Harris, H. (1969). The role of the nucleolus in the transfer of RNA from nucleus to cytoplasm. J. Cell Sci. *5*, 351–364.

Simard, R., and Bernhard, W. (1967). A heat-sensitive cellular function located in the nucleolus. J. Cell Biol. *74*, 794–815.

Siniossoglou, S., Wimmer, C., Rieger, M., Doye, V., Tekotte, H., Weise, C., Emig, S., Segref, A., and Hurt, E.C. (1996). A novel complex of nucleoporins, which includes Sec13p and a Sec13p homolog, is essential for normal nuclear pores. Cell *84*, 265–275.

Snow, C.M., Senior, A., and Gerace, L. (1987). Monoclonal antibodies identify a group of nuclear pore complex glycoproteins. J. Cell Biol. *104*, 1143–1156.

Strathmann, M., Hamilton, B.A., Mayeda, C.A., Simon, M.I., Meyerowitz, E.M., and Palazzolo, M.J. (1991). Transposon-facilitated DNA sequencing. Proc. Natl. Acad. Sci. USA *88*, 1247–1250.

Ward, W.W. (1979). Photochemical and Photobiological Reviews, vol. 4, ed. K.C. Smith, New York: Plenum Press, 1–57.

Wente, S.R., and Blobel, G. (1993). A temperature-sensitive *NUP116* null mutant forms a nuclear envelope seal over the yeast nuclear pore complex thereby blocking nucleocytoplasmic traffic. J. Cell Biol. *123*, 275–284.

Wente, S.R., and Blobel, G. (1994). NUP145 encodes a novel yeast glycine-leucine-phenylalanine-glycine (GLFG) nucleoporin required for nuclear envelope structure. J. Cell Biol. *125*, 955–969.

Wente, S.R., Rout, M.P., and Blobel, G. (1992). A new family of yeast nuclear pore complex proteins. J. Cell Biol. *119*, 705–723.

Wright, R., and Rhine, J. (1989). Transmission electron microscopy and immunocytochemical studies of yeast: analysis of HMG-CoA reductase overproduction by electron microscopy. Methods Cell Biol. *31*, 473–512.

Wu, J., Matunis, M.J., Kraemer, D., Blobel, G., and Coutavas, E. (1995). Nup358, a cytoplasmically exposed nucleoporin with peptide repeats, Ran-GTP binding sites, zinc fingers, a cyclophilin A homologous domain, and a leucine-rich region. J. Biol. Chem. *270*, 14209–14213.